New Jersey Institute of Technology
Digital Commons @ NJIT

Dissertations | Electronic Theses and Dissertations

Spring 5-31-1998

Performance improvements in wireless CDMA communications utilizing adaptive antenna arrays

Weichen Ye
New Jersey Institute of Technology

Follow this and additional works at: https://digitalcommons.njit.edu/dissertations

 Part of the Electrical and Electronics Commons

Recommended Citation

Ye, Weichen, "Performance improvements in wireless CDMA communications utilizing adaptive antenna arrays" (1998). *Dissertations*. 960.
https://digitalcommons.njit.edu/dissertations/960

This Dissertation is brought to you for free and open access by the Electronic Theses and Dissertations at Digital Commons @ NJIT. It has been accepted for inclusion in Dissertations by an authorized administrator of Digital Commons @ NJIT. For more information, please contact digitalcommons@njit.edu.

Copyright Warning & Restrictions

The copyright law of the United States (Title 17, United States Code) governs the making of photocopies or other reproductions of copyrighted material.

Under certain conditions specified in the law, libraries and archives are authorized to furnish a photocopy or other reproduction. One of these specified conditions is that the photocopy or reproduction is not to be "used for any purpose other than private study, scholarship, or research." If a, user makes a request for, or later uses, a photocopy or reproduction for purposes in excess of "fair use" that user may be liable for copyright infringement,

This institution reserves the right to refuse to accept a copying order if, in its judgment, fulfillment of the order would involve violation of copyright law.

Please Note: The author retains the copyright while the New Jersey Institute of Technology reserves the right to distribute this thesis or dissertation

Printing note: If you do not wish to print this page, then select "Pages from: first page # to: last page #" on the print dialog screen

NJIT New Jersey's Science & Technology University

The Van Houten library has removed some of the personal information and all signatures from the approval page and biographical sketches of theses and dissertations in order to protect the identity of NJIT graduates and faculty.

ABSTRACT

PERFORMANCE IMPROVEMENTS IN WIRELESS CDMA COMMUNICATIONS UTILIZING ADAPTIVE ANTENNA ARRAYS

by
Weichen Ye

This dissertation studies applications of adaptive antenna arrays and space-time adaptive processing (STAP) in wireless code-division multiple-access (CDMA) communications. The work addresses three aspects of the CDMA communications problems: (1) near-far resistance, (2) reverse link, (3) forward link. In each case, adaptive arrays are applied and their performance is investigated.

The near-far effect is a well known problem which affects the reverse link of CDMA communication systems. The near-far resistance of STAP is analyzed for two processing methods: maximal ratio combining and optimum combining. It is shown that while maximal ratio combining is not near-far resistant, optimum combining is near-far resistant when the number of cochannel interferences is less than the system dimensionality. The near-far effect can be mitigated by accurate power control at the mobile station. With practical limitations, the received signal power at a base station from a power-controlled user is a random variable due to power control error. The statistical model of signal-to-interference ratio at the antenna array output of a base station is presented, and the outage probability of the CDMA reverse link is analyzed while considering Rayleigh fading, voice activity and power control error. New analytical expressions are obtained and demonstrated by computer simulations. For the application of an adaptive antenna array at the forward link, a receiver architecture is suggested for the mobile station that utilizes a small two-antenna array for interference suppression. Such a receiver works well only when the channel vector of the desired signal is known. The identifying spreading codes (as in IS-95A for example) are used to provide an adaptive channel vector estimate, and control

the beam steering weight, hence improve the receiver performance. Numerical results are presented to illustrate the operation of the proposed receiver model and the improvement in performance and capacity.

PERFORMANCE IMPROVEMENTS IN WIRELESS CDMA COMMUNICATIONS UTILIZING ADAPTIVE ANTENNA ARRAYS

by
Weichen Ye

A Dissertation
Submitted to the Faculty of
New Jersey Institute of Technology
in Partial Fulfillment of the Requirements for the Degree of
Doctor of Philosophy

Department of Electrical and Computer Engineering

May 1998

Copyright © 1998 by Weichen Ye
ALL RIGHTS RESERVED

APPROVAL PAGE

PERFORMANCE IMPROVEMENTS IN WIRELESS CDMA COMMUNICATIONS UTILIZING ADAPTIVE ANTENNA ARRAYS

Weichen Ye

Dr. Alexander Haimovich, Dissertation Advisor — Date
Associate Professor of Electrical and Computer Engineering,
New Jersey Institute of Technology

Dr. Nirwan Ansari, Committee Member — Date
Professor of Electrical and Computer Engineering,
New Jersey Institute of Technology

Dr. Yeheskel Bar-Ness, Committee Member — Date
Distinguished Professor of Electrical and Computer Engineering,
New Jersey Institute of Technology

Dr. Hongya Ge, Committee Member — Date
Assistant Professor of Electrical and Computer Engineering,
New Jersey Institute of Technology

Dr. Stuart Schwartz, Committee Member — Date
Professor of Electrical Engineering,
Princeton University

BIOGRAPHICAL SKETCH

Author: Weichen Ye

Degree: Doctor of Philosophy

Date: May 1998

Undergraduate and Graduate Education:

- Doctor of Philosophy in Electrical Engineering,
  New Jersey Institute of Technology, Newark, NJ, 1998
- Master of Science in Electrical Engineering,
  Shanghai Jiao Tong University, Shanghai, P. R. China, 1991
- Bachelor of Science in Electrical Engineering,
  Shanghai Jiao Tong University, Shanghai, P. R. China, 1988

Major: Electrical Engineering

Presentations and Publications:

Weichen Ye and Alexander M. Haimovich
"Performance of Cellular CDMA with Cell Site Antenna Arrays, Rayleigh Fading, and Power Control Error," submitted to *IEEE Trans. on Communications*, May 1998

Weichen Ye and Alexander M. Haimovich
"Performance of a CDMA System with Space Diversity and Imperfect Power Control in Rayleigh Fading Environment," to appear in *Proceedings of IEEE 48th Vehicular Technology Conference*, Ottawa, Canada, May 1998.

Weichen Ye and Alexander M. Haimovich
"Outage Probability of Cellular CDMA System with Space Diversity, Rayleigh Fading and Power Control Error," *IEEE Communications Letters*, to appear.

Weichen Ye and Alexander M. Haimovich
"Probability of Bit Error in a Power Controlled Cellular CDMA System with Space Diversity," in *Proceedings of the 1998 Conference on Information Science and Systems*, Princeton, NJ, March 1998.

Weichen Ye, Yeheskel Bar-Ness and Alexander M. Haimovich
"A Mobile Station Receiver with Smart Antenna Canceller for Wireless CDMA Communications," in *Proceedings of the 1998 Symposium on Interference Rejection and Signal Separation in Wireless Communications*, Newark, NJ, March 1998.

Weichen Ye, Yeheskel Bar-Ness and Alexander M. Haimovich
"A Novel IS-95 CDMA Mobile Station Receiver Structure with Smart Antenna Canceller," submitted to *The 9th IEEE International Symposium on Personal, Indoor and Mobile Radio Communications*, Feb. 1998.

Weichen Ye, Yeheskel Bar-Ness and Alexander M. Haimovich
"Usage of Smart Antenna for Cancelling Neighboring Base-Station Interference in Wireless CDMA Communications," in *Proceedings of the 1997 Asilomar Conference on Signals, Systems, and Computers*, Pacific Grove, CA, Nov. 1997.

Weichen Ye, Xiao C. Bernstein and Alexander M. Haimovich
"Near-Far Resistance of Space-Time Processing for Wireless CDMA Communications," *IEEE Communications Letters*, Vol.1, No.4, July 1997.

Weichen Ye, Yeheskel Bar-Ness and Alexander M. Haimovich
"A Self-Correcting Loop for Joint Estimation-Calibration in Adaptive Radar," in *Proceedings of the 1997 IEEE National Radar Conference*, Syracuse, NY, May 1997.

Weichen Ye, Yeheskel Bar-Ness and Alexander M. Haimovich
"Adaptive Antenna Calibration at the Mobile for CDMA Communications," in *Proceedings of the 1997 Conference on Information Science and Systems*, Baltimore, MD, March 1997.

This dissertation is dedicated to my family

ACKNOWLEDGMENT

It was my pleasure to work under the supervision of my dissertation advisor, Professor Alexander Haimovich, over my Ph.D program. I greatly appreciate the inspiration I have received from Professor Haimovich, who introduced me to the field of adaptive signal processing.

I am deeply indebted to Professor Yeheskel Bar-Ness, whom I have learned from through courses, discussions, and research projects. I am most grateful to Professor Nirwan Ansari, Professor Hongya Ge, and Professor Stuart Schwartz, for their active participation in my dissertation committee and for their great comments.

Finally, I wish to express my appreciation to many of my present and former colleagues at the Center for Communications and Signal Processing Research at NJIT, for their support and encouragement.

TABLE OF CONTENTS

Chapter Page

LIST OF FIGURES

Figure Page

CHAPTER 1

INTRODUCTION

The 1990s have been described as the decade of wireless telecommunications. Along with the fast growth of wireless communications market, wireless communication technology has evolved from simple first-generation analog systems to second-generation digital systems with rich features and services for residential and business customers. The new version of communications for individuals, known as personal communications systems (PCS) will enable the network to deliver telecommunication services (voice, data, video, etc) without restrictions on the users' terminal, location in the work, point of access to the network, access technology, or transport method [1].

As second generation systems, both time-division multiple access (TDMA) and code-division multiple access (CDMA) are standardized and widely accepted. In particular, CDMA has demonstrated a capacity increase over the analog system, advanced mobile phone service (AMPS), of at least a factor of ten, which means only less than 1/10 base stations will be required when customers demand service increases [2]. CDMA also offers improved performance over TDMA based wireless networks [3, 4, 5, 6]. CDMA provides a superior, spectrally efficient, digital solution for cellular/PCS services. The CDMA air interface is near optimum in its use of the mobile station transmitter power, enabling the widespread use of low-cost, lightweight, hand-held portable units. The technology is also near optimum in its link budgets, minimizing the number of base stations required for a satisfactory grade of service coverage. The use of soft handoff nearly eliminates the annoyance of dropped calls, fading, and poor voice quality.

CDMA is a modulation and a multiple access technique based on spread-spectrum communications. Each signal consists of a different pseudo random binary

sequence that modulates a carrier, spreading the spectrum of the waveform. A large number of CDMA signals share the same frequency band. The signals are separated in the receiver by using a correlator that accepts only the signal from the selected binary sequence and despreads its spectrum. The other users' signals, whose codes do not match, are not despread and contribute only to the noise and represent interference generated by the system.

The increased demand for cellular/PCS service makes the industry under pressure to develop efficient systems with enhanced capability to support a larger number of subscribers on the limited frequency spectrum band. There are several ways to improve the capacity of a cellular/PCS system while maintaining a specified quality of service. One way is to decrease the frequency reuse factor and keep all other system parameters unchanged. Another way to increase system capacity is by shrinking cell size. The third one is to remove part or total interference power while effectively increase the signal-to-interference ratio [7].

In IS-95A cellular CDMA, the transmitting bandwidth is 1.25 MHz, and the same bandwidth is occupied by every cell, making the frequency reuse factor equal to one, thus reaching a limit which cannot be reduced. The second way mentioned above, shrinking cell size, raises system cost by requiring more base station equipments, which are very expensive, and also causes more frequent handoffs for fast moving mobile stations. For the third way, one of most important methods to reduce interference is to introduce spatial filtering into the system. Spatial filtering (adaptive beam forming) is now among the key components for performance improvement in the IMT-2000, the third generation universal wireless communications system. IMT-2000 will combine all of the possible advanced technologies used in fixed and mobile networks, including cordless, high and low mobility cellular/PCS, and mobile satellite technology. By exploiting the spatial domain via an adaptive

antenna array, the operational benefits to the network operator can be summarized as follows [8]:

1. Capacity enhancement

2. Coverage extension

3. Ability to support high data rates

4. Increased immunity to "near-far" problems

Adaptive array processing has been investigated and applied by the sonar and radar communities. It now appears that its ultimate technological home will be in wireless communications [9]. Applications of antenna arrays in wireless communications capture increasing amount of research in both academic institutions and industry [10, 11, 12, 13, 14, 15]. In a wireless communication system, a signal can travel from transmitter to receiver over multiple paths. This effect can cause fluctuations in the received signal's amplitude, phase, and angle of arrival, referred to as *multipath fading* [16]. Fading effects are commonly modeled as large-scale or small-scale, according to their rates of change over the spatial separation between transmitter and receiver. Large-scale fading represents the average signal power attenuation or path loss due to motion over large areas. This phenomenon is affected by prominent terrian features between the transmitter and receiver, known as *shadowing*. Small-scale fading refers to the rapid changes in signal amplitude and phase over a small spatial separation. If the multiple reflective paths are large in number and there is no line-of-sight signal component, the envelope of the received signal is statistically described by a Rayleigh distribution. When there is a dominant nonfading signal component present, such as a line-of-sight propagation path, the small-scale fading envelope is described by a Rician distribution [17]. In this dissertation, it is assumed that no dominant signal component is present, and

therefore, small-scale fading is referred to as *Rayleigh fading*. In direct sequence CDMA, multiple propagation paths can be exploited by the RAKE receiver [18]. The signal processing with adaptive antenna array and RAKE receiver is referred to as space-time adaptive processing (STAP). Maximal ratio combining (MRC) and optimum combining (OC) are two important techniques used for signal combining in both the space and time domains. With MRC, the signals received by an antenna array are combined to combat multipath Rayleigh fading of the desired signal. MRC provides the highest output signal-to-interference plus noise ratio (SINR) at the receiver when the interferences at each antenna element and at each RAKE finger are independent [19]. However, in a wireless communications scenario, the interfering signals presented at the antenna elements and the RAKE fingers are generally correlated. With OC, the received signals are weighted and combined to suppress interfering signals while combating desired signal fading, and hence, output SINR is maximized [10].

In wireless CDMA, it is possible for the strongest mobile station to capture the base station even when other mobile stations are also transmitting. Often the closest transmitter is able to capture the base station because of the small propagation path loss. This is called the *near-far* effect [20]. Receivers based on signal processing not susceptible to the near-far effect are known as near-far *resistant*. In recent years there has been considerable interest in the design and analysis of multiuser near-far resistant receivers [21, 22, 23, 24]. With current second generation CDMA systems, near-far effects are mitigated through power control. While this approach provides some relief, it is limited by practical considerations. STAP is a performance enhancement to single user detection which provides an alternative to multiuser detection. Since adaptive antennas have been suggested for the base stations of CDMA systems, the near-far resistance analysis of STAP is of high interest.

Due to the susceptibility of CDMA systems to the near-far problem, power control is the most important system requirement in current CDMA. The CDMA system capacity is maximized if each mobile transmitter power level is controlled so that its signal arrives at the base station with the minimum required signal-to-interference ratio (SIR) [20]. Generally, signal strength variation in path losses and shadowing effects is slow enough to be controlled, but variation due to Rayleigh fading is too rapid to be tracked by power control. However, based on the analysis [18] and experimental measurements [25], the received signal power at a base station from a power-controlled user varies according to a log-normal distribution with a standard deviation (power control error – PCE) on the order of 1.5 to 2.5 dB. Therefore, the total interference power is the power sum of multiple log-normal components. The computation of the distribution of a sum of log-normal random variables (RVs) has been examined in many publications [26, 27, 28, 29]. A closed form solution for the distribution is not known. However, Marlow gave a normal limit theorem for the power sum of independent RVs in [26], which showed that under very general conditions the power sum of independent random variables will be asymptotically normally distributed. Therefore, the common method used in these publications is to approximate the sum of log-normal RVs to another log-normal RV. Schwartz and Yeh presented an approximation technique for the evaluation of the mean and variance of the power sums with independent log-normal components [27]. In [28], Schwartz and Yeh's approach was extended for the case of correlated log-normal RVs. Another approximation introduced in [27] is Wilkinson's approach, which also approximates distribution of the power sum of log-normal RVs as normal, and then find the first two moments of the power sum. Several approaches that can be used to compute the distribution of a sum of log-normal RVs were investigated in [29], which showed that among the methods considered Wilkinson's approach could be the best method to compute the distribution of the sums of correlated log-normal RVs.

Adaptive antenna arrays along with RAKE receiver provide space-time processing to mitigate small-scale fading effects and utilize multiple paths in mobile communications. On two-way telephone conversations, numerous measurements have established that voice is active less than 50 percent of the time. To further reduce interference, a unique processing feature, voice activity gating, is added to the CDMA systems. This technique involves the monitoring of voice activity such that each transmitter is switched off during periods of no voice activity, thus cochannel interference (CCI) is reduced.

Since the scenario in mobile communications is very complicated, most of the research results about system performance only take into account some of the effects that were mentioned above. The performance analysis related to the log-normal interference can be found in [4, 5, 29, 30, 31, 32], however these results didn't take into account the effect of Rayleigh fading, and therefore cannot be extended to be used with space diversity techniques. The analysis of interference with both fading and shadowing has been considered in the recent publications [33, 34, 35, 36, 37, 38]. Unfortunately, some of the results were not in closed-forms, and others were approximations, which are generally not accurate enough to show the effect of small PCE. To predict the performance of CDMA systems, it is of great interest to be able to develop closed-form expressions which incorporate the effects of power control error, Rayleigh fading, voice activity and space-time processing.

While most of the publications explore the benefits of adaptive antenna arrays at the base station (reverse link receiver), it is also interesting to study the application of adaptive antenna arrays at the mobile station (forward link receiver). The capacity of wireless CDMA systems in the forward link is limited by both intra-cell and inter-cell cochannel interferences. In particular, if the mobile station is close to a cell boundary, the desired signal from the home base station is disturbed by relatively strong interference from neighboring base stations. The third generation wireless

communication systems are expected to support high bit rate wireless internet access, which raises the demand of capacity improvement in forward link. Antenna arrays have not been often suggested for the design of the mobile stations since the size of mobile limits effectiveness of space diversity. On the other hand, the antenna array with elements separated by an order of one half wavelength is particularly effective for interference suppression. Hence, it is a suitable candidate for mitigating inter-cell interference which strongly limits CDMA forward link performance.

Adaptive interference cancellers utilizing either known direction of signal arrival or known signal waveform structure have been analyzed in the past [39, 40]. The former, called the directionally constraint array, is the more suitable for use in point-to-point communications, but with substantial sensitivity to pointing errors [41, 42]. The latter canceller, in which the waveform reference is generated in the receiver using some known signal characteristics such as the code used in spread spectrum modulation was also developed for communication applications. A hybrid scheme using both types of constraints was suggested and a self-correcting of the pointing error was also shown in [43] to improve performance of a two-element array for spread spectrum analog communications. It uses the high SINR despread signal to provide a reference, which controls the phase of one of the inputs to the array. Another similar canceller based on Applebaum and Chapman model is the generalized sidelobe canceller (GSC). Its operation and steady state analysis were given in [44, 45]. Since the performance of this system also degrades due to pointing or random angle errors, a self-correcting loop in GSC for joint estimation-calibration in adaptive radar was proposed in [46], where a Doppler technique is used to provide cleaner reference of the desired signal for steering vector correction. These structures assume that the signals received at all antenna elements are with the same amplitudes but different phase delays. In a wireless communications scenario, however, the fading channels result in different amplitudes and phase delays of the signals among the antenna

elements with only one half wavelength separation. Therefore, the antenna arrays used in point-to-point communications and adaptive radar cannot be easily applied in wireless cellular/PCS communications.

The focus of this dissertation is to study the applications of adaptive antenna arrays in wireless CDMA communications. The contributions of this dissertation are summarized as follows:

1. Asymptotic efficiency and near-far resistance of STAP are analyzed and their closed-form expressions are derived for OC and MRC when the desired signal and cochannel interferers undergo frequency selective fading.

2. The performance of STAP is analyzed in terms of outage probability for instantaneous output SIR, and its closed-form approximation is derived while taking into account space-diversity, Rayleigh fading, voice activity and PCE. This performance measure is suitable for the communication which is sensitive to short-term SIR outage, such as high bit rate data communication.

3. When the system is used for voice transmission, a meaningful performance measure is the average SIR outage probability. A similar closed-form approximation of outage probability for average output SIR is obtained for this scenario.

4. Another important communications system performance, average probability of bit error, is also analyzed and its expression is derived.

5. The analyses of system performance (outage probability and probability of bit error) are extended to more general cases, which include other-cell interference, correlation of shadowing among different users, channel with time dispersion, pilot tone effect, and performance in terms of Erlang capacity.

6. To improve the wireless CDMA forward link capacity, a smart antenna receiver structure is proposed at the CDMA mobile station. A new algorithm is developed to adaptively control the beam steering weight and thus to improve the receiver performance (This work was done in collaboration with Professor Yeheskel Bar-Ness).

The rest of this dissertation is organized as follows: For reverse link, STAP in wireless CDMA base station is introduced and its near-far resistance in Rayleigh fading environment is analyzed in Chapter 2. New analytical results of outage probability and probability of bit error in reverse link are obtained in Chapter 3 while taking into account power control error, Rayleigh fading, voice activity and space diversity. For forward link, a smart antenna at the mobile station is proposed in Chapter 4 to mitigate interference and improve performance. Computer simulations are generated to verify the theoretical analyses in corresponding chapters. Finally, the conclusions are drawn in Chapter 5.

CHAPTER 2

SPACE-TIME PROCESSING AND NEAR-FAR RESISTANCE FOR WIRELESS CDMA COMMUNICATIONS

In a Rayleigh fading environment, direct sequence spread spectrum CDMA systems are not only resistant to multipath fading, but they can actually utilize the multipath components to improve the system performance. A RAKE receiver uses multipath correlators to separately detect the several strongest multipath components, which convey the same transmitted information signal, but with different time delays. The output of each correlator are weighted to provide a better estimate of the transmitted signal than is collected from any single component. Spatially separated antennas along with a RAKE receiver at the base station exploit signal information from both space and time domains, and provide space-time adaptive processing (STAP) in the receiver. This chapter introduces the STAP receiver model in CDMA reverse link, and analyzes its near-far resistance to cochannel interference (CCI). Both analytical and simulation results are presented.

2.1 Space-Time Adaptive Processing

Consider the reverse link of a CDMA cell, which serves $K+1$ active users, and uses a base station with an M-element antenna array. The channel is assumed to be frequency-selective with L resolvable paths. The fading is assumed slow, i.e., constant during the processing interval. Figure 2.1 shows the general configuration of the space-time receiver. The receiver consists of antenna elements with sufficient separation to provide for independent paths, and of tap-delay lines that align the multipath products. Assuming coherent carrier demodulation, the complex envelope of the signal received at the mth antenna element can be written as:

$$x_m(t) = \sum_{k=0}^{K} \sum_{l=0}^{L-1} c_{ml}^{(k)} g_k(t - lT_d - \tau_k) + v_m(t), \tag{2.1}$$

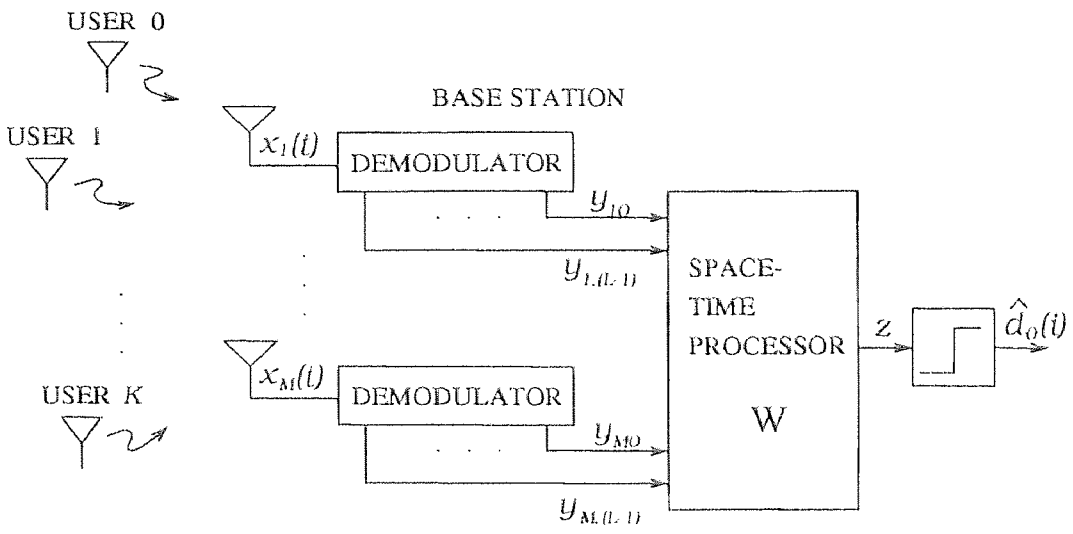

Figure 2.1 General configuration of the space-time CDMA receiver.

where the complex-valued scalars $c_{ml}^{(k)}$, $1 \leq m \leq M$, $0 \leq l \leq L-1$ represent the kth user channel coefficients, $g_k(t) = A_k' d_k(t) u_k(t)$, A_k' are the amplitudes of the different users, $d_k(t)$ are binary symbols, $u_k(t)$ are signature waveforms with unit energy[1], τ_k are the delays with respect to user 0 (desired user), and T_d represents the tap-delay in the channel model. Communication is to be carried out with user $k = 0$, while users $k = 1, \cdots, K$ supply the CCI. The desired user's delay τ_0 is assumed known to the receiver. The noise process $v_m(t)$ is complex-valued, circularly symmetric, white Gaussian with zero-mean and variance σ^2. In the context, matrices and vectors will be denoted by bold uppercase and bold lowercase letters, respectively.

Spread spectrum demodulation is applied at each antenna m and tap-delay l. At the end of the ith symbol interval, the demodulated output is given by

$$y_{ml}(i) = \int_{iT_s}^{(i+1)T_s} x_m(t + lT_d) u_0(t) dt, \tag{2.2}$$

where T_s is the symbol interval, $x_m(t)$ is measured at the lth tap-delay in the receiver, i.e., signal at the other taps lead with respect to $x_m(t)$. The outputs of the demodu-

[1]This model is not applicable to IS-95A, as the signature is the same for each symbol interval.

lators are stacked to form an ML dimensional vector, and are grouped according to components related to the desired user, interference and noise, yielding the expression (see [14] for details):

$$\mathbf{y}(i) = A_0 d_0(i)\mathbf{c}_0 + \mathbf{i}(i) + \mathbf{v}(i), \tag{2.3}$$

where A_0 and $d_0(i)$ are respectively the user's amplitude after demodulation and symbol, at the time under consideration. The vector $\mathbf{y}(i)$ can be written as

$$\mathbf{y}(i) = [y_{10}(i), y_{20}(i), \cdots, y_{M(L-1)}(i)]^T, \tag{2.4}$$

where "T" denotes transpose, $\mathbf{c}_0$ is the channel vector of the desired user, which can be given by

$$\mathbf{c}_0 = [c_{10}^{(0)}, c_{20}^{(0)}, \cdots, c_{M(L-1)}^{(0)}]^T, \tag{2.5}$$

and $\mathbf{v}(i)$ is the noise vector, with zero-mean and covariance matrix $E[\mathbf{v}(i)\mathbf{v}(i)^H] = \sigma^2\mathbf{I}$, where $\mathbf{I}$ is an $ML \times ML$ identity matrix. To simplify the ensuing analysis, it is assumed that self-interference terms are negligible, and that all sources are synchronized. In this case, the interference can be written as

$$\mathbf{i}(i) = \sum_{k=1}^{K} A_k d_k(i)\mathbf{c}_k, \tag{2.6}$$

where A_k is the amplitude of kth interference source after demodulation, and $\mathbf{c}_k$ is the channel coefficient vector of kth interference source. It is noted that the assumption of synchronized sources is not necessary, since if all signals have the same period, synchronization always exists between $d_0(i)$ and, at most, parts of two consecutive symbols of each cochannel interference. The output of the space-time processor is given by:

$$\begin{aligned} z(i) &= \mathbf{w}^H\mathbf{y}(i) \\ &= A_0 d_0(i)\mathbf{w}^H\mathbf{c}_0 + \mathbf{w}^H\mathbf{i}(i) + \mathbf{w}^H\mathbf{v}(i), \end{aligned} \tag{2.7}$$

where the superscript "H" denotes complex conjugate transpose, $\mathbf{w}$ is the weight vector determined by the combining criterion.

There are different criteria which can be used by the space-time processor to combine the signals. The weight vector that maximizes the signal-to-noise ratio (SNR) is simply the matched filter to the desired signal channel $\mathbf{c}_0$ [10, 19]. The combining method using this weight is referred to as maximal ratio combing (MRC). For MRC,

$$\mathbf{w} = \mathbf{c}_0. \tag{2.8}$$

When interference is present, MRC does not maximize signal-to-interference plus noise ratio (SINR), but joint domain optimum combining (OC) maximizes SINR at the array output [47]. For joint domain OC, the weight vector is given by

$$\mathbf{w} = \mathbf{R}^{-1}\mathbf{c}_0, \tag{2.9}$$

where $\mathbf{R}$ is the interference and noise covariance matrix, and can be expressed as:

$$\mathbf{R} = E\left[(\mathbf{i}(i) + \mathbf{v}(i))(\mathbf{i}(i) + \mathbf{v}(i))^H\right]. \tag{2.10}$$

2.2 Near-Far Resistance of STAP

Near-far resistance is one of the performance measures of CDMA receivers. In conventional single-user detection, the receiver at the base station consists of a group of demodulators, for each user. Obviously, the single-user detector suffers from the near-far problem when the CDMA signature sequences are not orthogonal. Multiuser detection uses information about multiple users to improve detection of each individual user. Multiuser detectors were studied extensively to overcome the near-far problem in CDMA communications [23].

STAP can be applied to mitigate fading of desired signal as well as suppress CCI in wireless CDMA communications [13, 14]. STAP followed by single-user detection provides an alternative to the multiuser detectors for performance improvement of the current CDMA systems. In this section, the near-far resistance of STAP is investigated for joint domain MRC and OC processing.

Performance degradation due to the presence of CCI can be quantified by the *asymptotic efficiency* [21]. Let γ denote the user output SNR in the absence of CCI. Using (2.7), γ can be written as

$$\gamma = \frac{A_0^2 |\mathbf{w}^H \mathbf{c}_0|^2}{\sigma^2 \|\mathbf{w}\|^2}, \tag{2.11}$$

where $\|\mathbf{w}\|^2 = \mathbf{w}^H \mathbf{w}$. In a coherent binary phase-shift keying (BPSK) system, the bit error rate (BER) is a function of output SNR [17]:

$$P_e = Q\left(\sqrt{\gamma}\right), \tag{2.12}$$

where $Q(\cdot)$ is the Gaussian tail function, defined by [48]

$$Q(x) = \frac{1}{\sqrt{2\pi}} \int_x^\infty e^{-t^2/2} dt.$$

In the presence of CCI, for the same power of the desired signal, the BER $P_e > Q(\sqrt{\gamma})$. The effective SNR γ_e is defined as the SNR required to achieve the BER $P_e = Q(\sqrt{\gamma_e})$. The ratio γ_e/γ represents the performance loss due to CCI. Then the asymptotic efficiency is defined as [22, 17]:

$$\eta = \lim_{\sigma^2 \to 0} \frac{\gamma_e}{\gamma}. \tag{2.13}$$

As the noise tends to zero, the effective SNR γ_e becomes dependent on the interference term $\mathbf{i}(i)$. By convention, the asymptotic efficiency is defined such that the interference resultant $\mathbf{i}(i)$ reduces the user's signal (when the transmitted bit is positive). Thus the effective SNR is expressed as

$$\gamma_e = \frac{E\left[\max(0, A_0 |\mathbf{w}^H \mathbf{c}_0| - |\mathbf{w}^H \mathbf{i}(i)|)\right]^2}{\sigma^2 \|\mathbf{w}\|^2}, \tag{2.14}$$

where the expectation operator "E" is with respect to the background noise and the interference, but is conditioned on the channel vectors. Therefore, the asymptotic efficiency is:

$$\eta = \lim_{\sigma^2 \to 0} \frac{E\left[\max(0, |\mathbf{w}^H \mathbf{c}_0| - |\mathbf{w}^H \mathbf{i}(i)|/A_0)\right]^2}{\|\mathbf{c}_0\|^2 \|\mathbf{w}\|^2}. \tag{2.15}$$

The near-far resistance $\overline{\eta}$ is a performance measure that captures the system performance under worst-case conditions; it is defined as the greatest lower bound of the asymptotic efficiency over all possible combinations of power, channel vectors and interference bits, $\overline{\eta} = \inf\ \eta$ [22]. Worst-case conditions are specified as follows:

1. Channel vectors representing CCI form an orthogonal set, which can be expressed as:

$$\mathbf{c}_k^H \mathbf{c}_j = \|\mathbf{c}_k\|^2 \delta_{kj}, \quad k, j = 1, \cdots, K, \quad K \leq ML, \tag{2.16}$$

where

$$\delta_{kj} = \begin{cases} 1, & k = j \\ 0, & k \neq j \end{cases}. \tag{2.17}$$

In this case, each source consumes exactly one degree of freedom.

2. All interferences combine coherently to reduce the desired signal, i.e., the effective amplitude is given by $A_0|\mathbf{w}^H\mathbf{c}_0| - \sum_{k=1}^{K} A_k|\mathbf{w}^H\mathbf{c}_k|$.

3. The interference power goes to infinity, $A_k \to \infty$.

Under above conditions, the near-far resistance can then be expressed as:

$$\overline{\eta} = \lim_{\substack{\sigma^2 \to 0 \\ A_k \to \infty}} \frac{\left[\max\left(0, |\mathbf{w}^H\mathbf{c}_0| - \sum_{k=1}^{K} \frac{A_k|\mathbf{w}^H\mathbf{c}_k|}{A_0}\right)\right]^2}{\|\mathbf{c}_0\|^2 \|\mathbf{w}\|^2}. \tag{2.18}$$

Since MRC ignores CCI, it is not expected to be near-far resistant. Indeed, for $\mathbf{w} = \mathbf{c}_0$, the near-far resistance is given by

$$\begin{aligned} \overline{\eta}_{\text{mrc}} &= \lim_{\substack{\sigma^2 \to 0 \\ A_k \to \infty}} \frac{\left[\max\left(0, |\mathbf{c}_0^H\mathbf{c}_0| - \sum_{k=1}^{K} \frac{A_k|\mathbf{c}_0^H\mathbf{c}_k|}{A_0}\right)\right]^2}{\|\mathbf{c}_0\|^2 \|\mathbf{c}_0\|^2} \\ &= \lim_{\substack{\sigma^2 \to 0 \\ A_k \to \infty}} \left[\max\left(0, 1 - \sum_{k=1}^{K} \frac{A_k|\mathbf{c}_0^H\mathbf{c}_k|}{A_0\|\mathbf{c}_0\|^2}\right)\right]^2 \\ &= 0. \end{aligned} \tag{2.19}$$

The MRC is clearly not near-far resistant.

Joint domain OC maximizes SINR at array output even when interference is present. The weight vector of joint domain OC is written by

$$\mathrm{w} = \mathbf{R}_K^{-1}\mathrm{c}_0, \tag{2.20}$$

where $\mathbf{R}_K$ is the interference and noise covariance matrix associated with the K CCI sources [14]:

$$\begin{aligned}\mathbf{R}_K &= E\left[(\mathrm{i}(i)+\mathrm{v}(i))(\mathrm{i}(i)+\mathrm{v}(i))^H\right] \\ &= \sum_{k=1}^{K} A_k^2\mathrm{c}_k\mathrm{c}_k^H + \sigma^2\mathbf{I}.\end{aligned} \tag{2.21}$$

It is easy to show that $A_k^2\left\|\mathrm{c}_k\right\|^2$ and $\frac{\mathrm{c}_k}{\|\mathrm{c}_k\|}$ are the principal eigenvalues and eigenvectors of $\mathbf{R}_K$, respectively. Utilizing the result in [49, 50], we have the inverse of matrix $\mathbf{R}_K$ as:

$$\mathbf{R}_K^{-1} = \frac{1}{\sigma^2}\left(\mathbf{I} - \sum_{k=1}^{K}\frac{A_k^2\mathrm{c}_k\mathrm{c}_k^H}{\sigma^2 + A_k^2\left\|\mathrm{c}_k\right\|^2}\right). \tag{2.22}$$

The near-far resistance, as defined in (2.18), is invariant to gain factor in the weight vector w. Using (2.20) and (2.22), and ignoring the $1/\sigma^2$ gain factor, the weight vector is given by

$$\mathrm{w} = \mathrm{c}_0 - \sum_{k=1}^{K}\frac{A_k^2\mathrm{c}_k\mathrm{c}_k^H}{\sigma^2 + A_k^2\left\|\mathrm{c}_k\right\|^2}\mathrm{c}_0. \tag{2.23}$$

As $\sigma^2 \to 0$, the weight vector can be expressed by

$$\lim_{\sigma^2\to 0}\mathrm{w} = \mathrm{c}_0 - \sum_{k=1}^{K}\frac{\mathrm{c}_k\mathrm{c}_k^H}{\left\|\mathrm{c}_k\right\|^2}\mathrm{c}_0. \tag{2.24}$$

From this expression, and after some algebra (see Appendix A for details), one obtains

$$\lim_{\sigma^2\to 0}\left\|\mathrm{w}\right\|^2 = \left\|\mathrm{c}_0\right\|^2 - \sum_{k=1}^{K}\frac{\left|\mathrm{c}_0^H\mathrm{c}_k\right|^2}{\left\|\mathrm{c}_k\right\|^2}. \tag{2.25}$$

Substituting (2.24) and (2.25) in (2.18), and after some algebraic manipulations (see Appendix A for details), the near-far resistance of joint domain OC is given by

$$\overline{\eta} = 1 - \sum_{k=1}^{K}\frac{\left|\mathrm{c}_0^H\mathrm{c}_k\right|^2}{\left\|\mathrm{c}_0\right\|^2\left\|\mathrm{c}_k\right\|^2}. \tag{2.26}$$

To obtain an expression for $\overline{\overline{\eta}}$ independent of the channels, it is assumed that $\mathbf{c}_0$, $\mathbf{c}_k$ are random vectors independently distributed as $\mathcal{CN}[\mathbf{0}, \mathbf{I}]$, where the symbol $\mathcal{CN}$ stands for the complex-valued normal distribution. The near-far resistance averaged over the channels is given by:

$$\begin{aligned} \overline{\overline{\eta}} &= E_{\mathbf{c}_0, \mathbf{c}_k}[\overline{\eta}] \\ &= E_{\mathbf{c}_0, \mathbf{c}_k}\left[1 - \sum_{k=1}^{K} \frac{|\mathbf{c}_0^H \mathbf{c}_k|^2}{\|\mathbf{c}_0\|^2 \|\mathbf{c}_k\|^2}\right]. \end{aligned} \tag{2.27}$$

In [51] it was shown that

$$E_{\mathbf{c}_0, \mathbf{c}_k}\left[\frac{|\mathbf{c}_0^H \mathbf{c}_k|^2}{\|\mathbf{c}_0\|^2 \|\mathbf{c}_k\|^2}\right] = \frac{1}{ML}, \tag{2.28}$$

hence for $K \leq ML$, the near-far resistance can be written as

$$\overline{\overline{\eta}} = 1 - \frac{K}{ML}, \tag{2.29}$$

or for an arbitrary K, it is

$$\overline{\overline{\eta}} = \max\left(0, 1 - \frac{K}{ML}\right). \tag{2.30}$$

In the absence of CCI, all available ML degrees of freedom can be applied to diversity processing. In the worst-case, each interference source consumes one complete degree of freedom. Since the space-time architecture has ML degrees of freedom, STAP is near-far resistant as long as the number of interference sources is less than the signal space dimensionality.

2.3 Numerical Results

Computer simulations are used to verify the analyses in the last section. Figure 2.2 shows the asymptotic efficiency of space-time processing for 1, 2, 4, and 8 interference sources respectively, with processing gain of 127, and system dimension $ML = 8$. The curves were generated using (2.15) and realizations of channel vectors $\mathbf{c}_0$, $\mathbf{c}_k$

distributed as $\mathcal{CN}[\mathbf{0},\mathbf{I}]$. All interference sources have the same power level at the base station. The abscissa of the plot is SNRi-SNRo where, SNRi is the input interference-to-noise power ratio per channel, and SNRo denotes the input desired signal-to-noise ratio per channel. Curves shown are averages of 200 Monte Carlo runs. The simulation demonstrates that MRC is not near-far resistant, but OC is near-far resistant with the loss of one degree of freedom for each interference source. When the number of interference sources reaches the system dimension, OC is no longer near-far resistant. The near-far resistance clearly serves as a lower bound for the asymptotic efficiency.

The BER expressed in (2.12) is conditioned on the SNR γ. The BER, when γ is random, can be obtained by taking the average over the probability density function of γ. Thus the average BER of the system is given by [17]:

$$P_b = \int_0^\infty P_e(\gamma) f(\gamma) d\gamma, \tag{2.31}$$

where $f(\gamma)$ is the probability density function of γ. Figure 2.3 shows simulation curves of the BER for both MRC and OC. For $K = ML$ interference sources and using OC, the BER increases dramatically close 0.5 as the power of interference sources increases. The system is clearly near-far resistant for $K < ML$.

2.4 Summary

STAP in CDMA reverse link receiver was introduced and its near-far resistance was analyzed when applying MRC and OC. Both analytical and simulation results show that while MRC is not near-far resistant, OC is near-far resistant when the number of CCI sources is less than the system dimensionality. Generally, there are dozens of interfering signals present in a CDMA system, therefore, power control is still a key requirement in CDMA even when STAP with OC is applied. In the case that the system fails in the power control of a few number of reverse link signals (less than

system dimensionality), the STAP with OC can relief the effect of strong interference and thus improve the system performance.

The CDMA reverse link performance will be investigated further in the next chapter when the power control is imperfect.

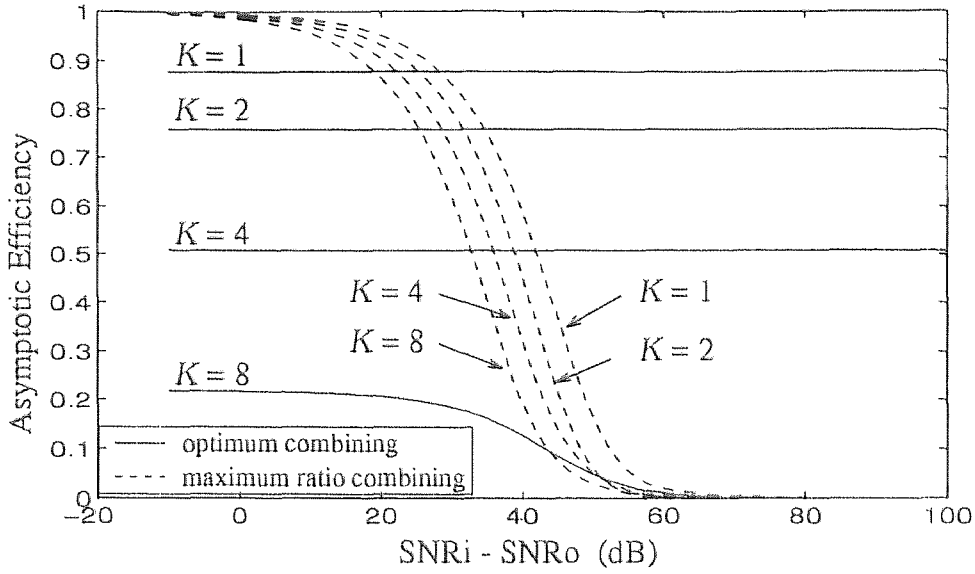

Figure 2.2 Asymptotic efficiency of an antenna array with system dimension $ML = 8$, K is the number of interference sources.

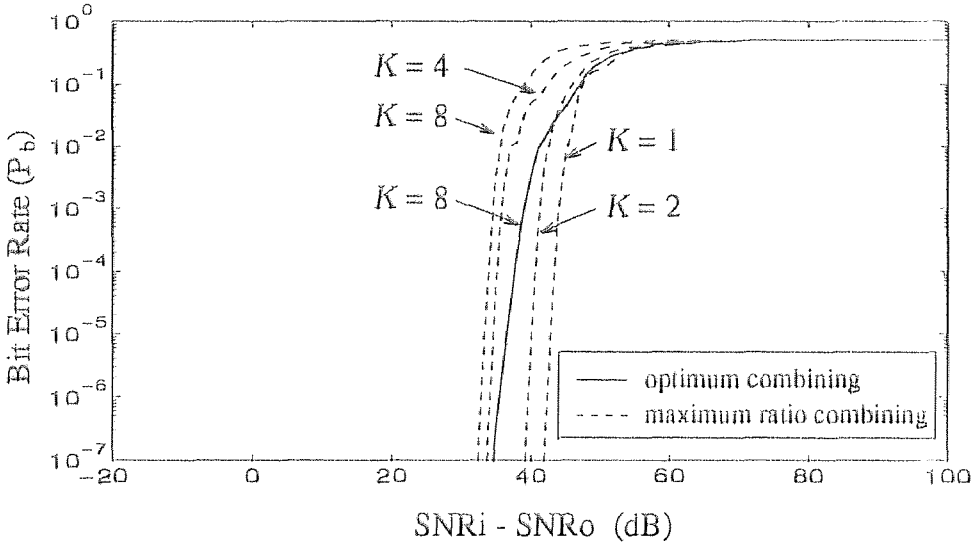

Figure 2.3 Bit error rate of a CDMA receiver with system dimension $ML = 8$, K is the number of interference sources.

CHAPTER 3

PERFORMANCE OF CELLULAR CDMA WITH CELL SITE ANTENNA ARRAYS FOR FREQUENCY-SELECTIVE FADING AND POWER CONTROL ERROR

In Chapter 2, the near-far resistance of STAP was studied. It was shown by both analyses and simulations that STAP in wireless CDMA is generally not near-far resistant, while STAP with OC can mitigate the effect of a few strong interferences. The solution to the near-far problem is still the use of power control, which attempts to ensure that all signals from the mobile stations within a given cell arrive at the base station of that cell with equal power. The primary motivation of power control is to maximize capacity, an additional benefit being to mobile station power conservation. As stated in Chapter 1, power control accuracy is limited by practical considerations. The effect of power control error (PCE) results in degradation of system performance and capacity. This chapter details the performance and capacity analysis of a wireless CDMA system while taking into account the PCE, Rayleigh fading, voice activity and STAP.

3.1 System Model

The system model represents the reverse link of a single cell CDMA system which serves K_u users, and uses a base station with an M-element antenna array. The received signals are assumed to undergo independent Rayleigh fading, and only one path for each user's signal is present. It is further assumed that the fading is flat and slowly varying such that the lowpass equivalent channel seen by each antenna can be characterized by a complex-valued scalar. The system is assumed interference limited with negligible thermal noise. The CDMA reverse link receiver model is shown in Figure 3.1. The complex envelope of the signal received at the base station is then expressed by an M-dimensional vector:

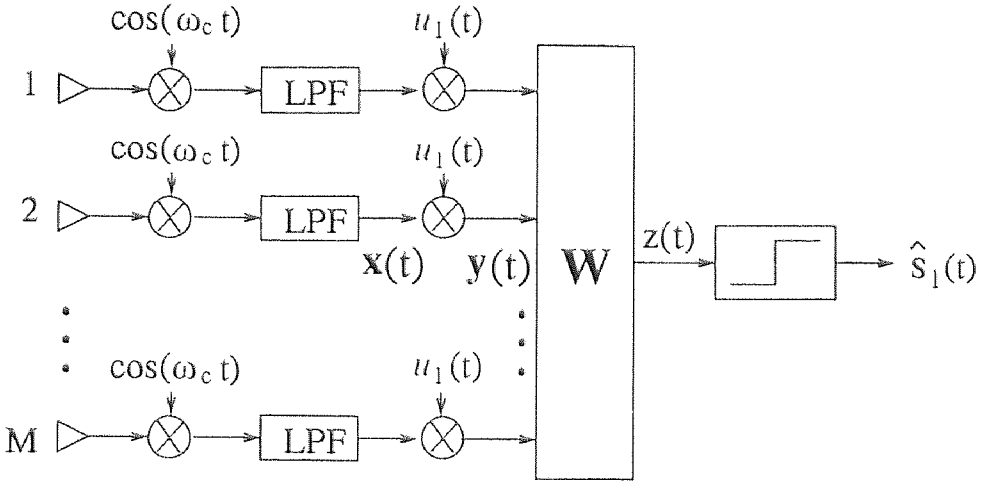

Figure 3.1 CDMA reverse link receiver model

$$\mathbf{x}(t) = \sqrt{\lambda_1}\, s_1(t-\tau_1)u_1(t-\tau_1)\mathbf{c}_1 + \sum_{k=2}^{K_u} \epsilon_k \sqrt{\lambda_k}\, s_k(t-\tau_k)u_k(t-\tau_k)\mathbf{c}_k, \qquad (3.1)$$

where the first and second terms respectively represent the desired signal and the CCI, λ_k $(k = 1, \cdots, K_u)$ are the powers of the received signals, $\mathbf{c}_k$ are normalized complex Gaussian channel vectors with $E\left[\mathbf{c}_k \mathbf{c}_k^H\right] = \mathbf{I}$, $\mathbf{I}$ is the $M \times M$ identity matrix, the superscript denotes transpose and complex conjugate, $s_k(t)$ are NRZ waveforms of the users' data, $u_k(t)$ are the spreading sequences, ϵ_k are binary random variables indicating the users' voice activities, and τ_k are the users' delays. Let $s_k(t) = \sum_i s_k(i)\, h(t - iT_s)$, where $h(t)$ is the basic pulse shape, T_s is the symbol interval, and $s_k \in \{-1, 1\}$ are the users' binary data with $E[s_k(i)] = 0$, and $E[s_k(i)\, s_l(j)] = \delta_{kl}\delta_{ij}$, where $\delta_{ij} = 1$ for $i = j$, and $\delta_{ij} = 0$ otherwise. The signature waveforms are normalized to unit energy over the symbol interval. For convenience, $\tau_1 = 0$. In a system with perfect power control, all λ_k's are equal. The received powers λ_k are the result of path loss, shadowing and imperfect power control, and are modeled as independent identically distributed (i.i.d.) random variables with log-normal distribution, but the values of λ_k change slowly compared to Rayleigh

fading. If λ_k's have a log-normal distribution, then $\alpha_k = 10\log_{10}\lambda_k$ are normal. The standard deviation of α_k is the PCE measured in dB. The voice activity ϵ_k is modeled as a Bernoulli (p) random variable with $\Pr(\epsilon_k = 1) = p$, where p is the *voice activity factor*.

Following spread spectrum demodulation and sampling at the symbol interval, the received signal can be written:

$$\begin{aligned} \mathbf{y}(i) &= \int_{iT_s}^{(i+1)T_s} \mathbf{x}(t)u_1(t)dt \\ &= \sqrt{\lambda_1}s_1(i)\mathbf{c}_1 + \sum_{k=2}^{K_u} \epsilon_k\sqrt{\lambda_k}\left(s_k(i-1)\rho_k^- + s_k(i)\rho_k^+\right)\mathbf{c}_k, \end{aligned} \tag{3.2}$$

where $\rho_k^- = \int_{iT_s}^{iT_s+\tau_k} u_k(t-\tau_k)u_1(t)dt$, and $\rho_k^+ = \int_{iT_s+\tau_k}^{(i+1)T_s} u_k(t-\tau_k)u_1(t)dt$ are the correlations between user signatures. User signatures may be supplied by a long code such as in IS-95A, however it is assumed that the correlations above are independent of the symbol interval index i.

The antenna array outputs $\mathbf{y}(i)$ are combined using the method of maximal ratio combining (MRC). The array weight vector $\mathbf{w}$ then acts as a channel matched filter, $\mathbf{w} = \mathbf{c}_1$. The array output is expressed:

$$\begin{aligned} z(i) &= \mathbf{w}^H\mathbf{y}(i) = \mathbf{c}_1^H\mathbf{y}(i) \\ &= \phi_s(i) + \phi_j(i), \end{aligned} \tag{3.3}$$

where

$$\phi_s(i) = \sqrt{\lambda_1}s_1(i)\mathbf{c}_1^H\mathbf{c}_1 \tag{3.4}$$

and

$$\phi_j(i) = \mathbf{c}_1^H\sum_{k=2}^{K_u}\epsilon_k\sqrt{\lambda_k}\left(s_k(i-1)\rho_k^- + s_k(i)\rho_k^+\right)\mathbf{c}_k \tag{3.5}$$

are the desired signal and CCI respectively, at the array output. Over the duration of a bit, it is assumed that the interference can be approximated by an equivalent source using the following expression:

$$\phi_j(i) = s(i)\mathbf{c}_1^H\sum_{k=2}^{K_u}\epsilon_k\sqrt{\eta_k\lambda_k}\,\mathbf{c}_k, \tag{3.6}$$

where $s(i)$ combines the total interference bit effects during the bit duration and η_k is a gain factor incorporating the effect of cross-correlation with the desired user's signal. This model is a worst case of sorts, in which it is not assumed independence among the interference sources. This model has the advantage of being tractable analytically (see also [10]). The instantaneous output SIR is written as:

$$\gamma = \frac{P_s}{P_J}, \tag{3.7}$$

where P_s and P_J are respectively the desired signal and interference powers. Utilizing the expressions in (3.4) and (3.6), P_s and P_J are given by:

$$P_s = \lambda_1 \left| \mathbf{c}_1^H \mathbf{c}_1 \right|^2, \tag{3.8}$$

$$P_J = \left| \mathbf{c}_1^H \sum_{k=2}^{K_u} \epsilon_k \sqrt{\eta_k \lambda_k}\, \mathbf{c}_k \right|^2. \tag{3.9}$$

In the next section, the system performance is based on this signal model.

3.2 Analysis of PCE and Fading Effects

In this section, relations are established for performance measures such as outage and bit error rate, as functions of PCE and other system parameters. The outage probability is defined as the probability that the output SIR falls below a prescribed level. The analysis is carried out for two different definitions of the outage. The first case studied is outage of the *instantaneous* SIR. This definition befits the case of data transmission, where even a brief outage may affect performance. Alternatively, outage may be defined with respect to the SIR *averaged* over Rayleigh fading. This approach is suitable for voice transmission, as the human ear will detect only longer duration outages.

3.2.1 Outage Probability of Instantaneous SIR

In the first case, the goal is to compute the instantaneous SIR outage averaged over Rayleigh fading, PCE, and voice activity. Utilizing the signal model in Section 3.1,

the instantaneous SIR is given by:

$$\gamma = \frac{\lambda_1 \left| \mathbf{c}_1^H \mathbf{c}_1 \right|^2}{\left| \mathbf{c}_1^H \sum_{k=2}^{K_u} \epsilon_k \sqrt{\eta_k \lambda_k}\, \mathbf{c}_k \right|^2}. \tag{3.10}$$

The cumulative distribution function of γ conditioned on the input SIR μ was found in [19, 10]

$$F(\gamma \mid \mu) = \frac{(\gamma/\mu)^M}{(1+\gamma/\mu)^M}, \tag{3.11}$$

where

$$\mu = \frac{\lambda_1}{\sum_{k=2}^{K_u} \epsilon_k \eta_k \lambda_k}. \tag{3.12}$$

It is noted that the input SIR μ is a function of the shadowing λ_k and the voice activity ϵ_k, and hence is a random variable. To fully characterize the outage probability, it is desired to obtain the density function of μ. Let $\mathcal{I}$ denote the interference power, then from (3.12)

$$\mathcal{I} = \sum_{k=2}^{K_u} \epsilon_k \eta_k \lambda_k. \tag{3.13}$$

Since $\epsilon_k \in \{0, 1\}$, $\mathcal{I}$ is the sum of log-normal random variables. The number of elements in the sum is $\sum_{k=2}^{K_u} \epsilon_k$. A method to approximate the distribution of a sum of log-normal random variables based on cumulant matching was introduced in [27, 29]. The method assumes that $\mathcal{I}$ is log-normal; it then proceeds to match $E[\mathcal{I}]$ and $E[\mathcal{I}^2]$ computed from (3.13) with the corresponding cumulants of the log-normal distribution. Consistent with the assumption that $\mathcal{I}$ is log-normal, it can be expressed as $\mathcal{I} = e^b$, where b has a normal distribution, $b \sim \mathcal{N}[m_b, \sigma_b^2]$, where the mean m_b and the variance σ_b^2 are to be determined. It follows that

$$E[\mathcal{I}] = E\left[e^b\right] = e^{m_b + \sigma_b^2/2}, \tag{3.14}$$

$$E\left[\mathcal{I}^2\right] = E\left[e^{2b}\right] = e^{2m_b + 2\sigma_b^2}. \tag{3.15}$$

Let the user powers λ_k be expressed in terms of the normal random variables $a_k \sim \mathcal{N}[m_a, \sigma_a^2]$, $\lambda_k = e^{a_k}$. The random variable a_k is related to the quantity α_k defined

in the Section 3.1,

$$a_k = \alpha_k (\ln 10)/10. \tag{3.16}$$

From (3.13), and taking the expectation over ϵ_k and a_k,

$$\begin{aligned} E[\mathcal{I}] &= E\left[\sum_{k=2}^{K_u} \epsilon_k \eta_k e^{a_k}\right] = \sum_{k=2}^{K_u} \eta_k E[\epsilon_k] E[e^{a_k}] \\ &= p e^{m_a + \sigma_a^2/2} \sum_{k=2}^{K_u} \eta_k \equiv e^{\xi_1}. \end{aligned} \tag{3.17}$$

Similarly,

$$\begin{aligned} E[\mathcal{I}^2] &= E\left[\left(\sum_{k=2}^{K_u} \epsilon_k \eta_k e^{a_k}\right)^2\right] \\ &= \sum_{k=2}^{K_u} \eta_k^2 E\left[\epsilon_k^2 e^{2a_k}\right] + 2\sum_{k=2}^{K_u} \sum_{j=k+1}^{K_u} \eta_k \eta_j E\left[\epsilon_k e^{a_k} \epsilon_j e^{a_j}\right] \\ &= p e^{2m_a + 2\sigma_a^2} \sum_{k=2}^{K_u} \eta_k^2 + p^2 e^{2m_a + \sigma_a^2} \sum_{k=2}^{K_u} \sum_{j \neq k} \eta_k \eta_j \equiv e^{\xi_2}. \end{aligned} \tag{3.18}$$

By equating (3.14) with (3.17) and (3.15) with (3.18), the unknown quantities m_b, σ_b^2 can be expressed

$$m_b = 2\xi_1 - \frac{1}{2}\xi_2 \tag{3.19}$$

$$\sigma_b^2 = \xi_2 - 2\xi_1. \tag{3.20}$$

Now, from (3.12) and the log-normality of λ_1 and $\mathcal{I}$, it follows that μ is also log-normal. Indeed,

$$g = \ln \mu = \ln \frac{\lambda_1}{\mathcal{I}} = a_1 - b, \tag{3.21}$$

is normal, and hence $\mu = e^g$ is log-normal. The density function of μ is determined from the mean and variance of g:

$$m_g = m_a - m_b, \tag{3.22}$$

$$\sigma_g^2 = \sigma_a^2 + \sigma_b^2. \tag{3.23}$$

Thus all the ingredients required to compute the density function of μ are available.

The outage probability is defined as the probability P_o that the output SIR γ, falls below a threshold ζ, $P_o = \Pr(\gamma < \zeta)$. The outage probability conditioned on the input SIR μ is given by (3.11),

$$\begin{aligned} P_o(\mu) &= F(\gamma = \zeta) \\ &= \frac{(\zeta/\mu)^M}{(1+\zeta/\mu)^M} . \end{aligned} \tag{3.24}$$

The outage probability averaged over Rayleigh fading, PCE and voice activity is given by

$$P_o = \int_0^\infty P_o(\mu) f(\mu) d\mu \tag{3.25}$$

or since $\mu = e^g$,

$$P_o = \int_{-\infty}^\infty P_o(g) f(g) dg = E_g \left[P_o(g) \right], \tag{3.26}$$

where

$$P_o(g) = \frac{(\zeta e^{-g})^M}{(1+\zeta e^{-g})^M}. \tag{3.27}$$

An exact closed-form expression for the integral in (3.26) is not available, however an approximation exists for $E_g \left[P_o(g) \right]$ when g is normal. The approximation is for an arbitrary function $P_o(g)$ and is expressed in terms of the mean m_g and the standard deviation σ_g [52]:

$$\begin{aligned} P_o &= E_g \left[P_o(g) \right] \\ &\cong \frac{2}{3} P_o(m_g) + \frac{1}{6} P_o\left(m_g + \sqrt{3}\,\sigma_g\right) + \frac{1}{6} P_o\left(m_g - \sqrt{3}\,\sigma_g\right). \end{aligned} \tag{3.28}$$

The previous relation provides for the closed-form computation of the average outage probability derived from the instantaneous SIR as a function of Rayleigh fading, PCE, and voice activity.

3.2.2 Outage Probability of Average SIR

The outage probability provides an indicator of how often the communication link's quality is under a specified acceptable level. The system capacity is generally

computed for a set outage. When the mobiles transmit voice rather than data, it is more suitable to consider longer duration outages. In this case it is better to define the outage with respect to the SIR averaged over the Rayleigh fading. We proceed to determine the average power of the signal and interference.

Given the vector of channel coefficients $\mathbf{c}_1 = [c_{11}, \cdots, c_{1M}]^T$, where c_{1m} $(m = 1, \cdots, M)$ are independent complex Gaussian random variables with zero mean and $E[|c_{1m}|^2] = 1$, the average signal power at the array output is expressed:

$$\begin{aligned} S &= E\left[\lambda_1 \left|\mathbf{c}_1^H \mathbf{c}_1\right|^2\right] \\ &= \lambda_1 E\left[\left(\sum_{m=1}^{M} |c_{1m}|^2\right)^2\right]. \end{aligned} \tag{3.29}$$

It can be shown that (see Appendix B for details)

$$S = \left(M^2 + M\right)\lambda_1. \tag{3.30}$$

The average interference power at the array ouput is given by:

$$J = E\left[\left|\mathbf{c}_1^H \left(\sum_{k=2}^{K_u} \epsilon_k \sqrt{\eta_k \lambda_k}\, \mathbf{c}_k\right)\right|^2\right]. \tag{3.31}$$

The vector $\sum_{k=2}^{K_u} \epsilon_k \sqrt{\eta_k \lambda_k}\, \mathbf{c}_k$ has a complex Gaussian distribution with zero mean and covariance matrix $\mathcal{I}\,\mathbf{I}$, where $\mathcal{I}$ was defined in (3.13), and $\mathbf{I}$ is the identity matrix. It follows that one can set

$$\sum_{k=2}^{K_u} \epsilon_k \sqrt{\eta_k \lambda_k}\, \mathbf{c}_k = \sqrt{\mathcal{I}}\, \mathbf{c}_p, \tag{3.32}$$

where $\mathbf{c}_p = [c_{p1}, \cdots, c_{pM}]^T$ is complex Gaussian with zero mean and $E[\mathbf{c}_p \mathbf{c}_p^H] = \mathbf{I}$. The average interference power can then be written as (see Appendix B for details):

$$\begin{aligned} J &= \mathcal{I}\, E\left[\left|\mathbf{c}_1^H\, \mathbf{c}_p\right|^2\right] \\ &= M\mathcal{I}. \end{aligned} \tag{3.33}$$

The average SIR can be expressed as:

$$\gamma_E = \frac{S}{J} = (M+1)\frac{\lambda_1}{\mathcal{I}} = (M+1)\mu. \tag{3.34}$$

The outage is now defined as the probability that γ_E falls below a threshold ζ_E: $P_{oE} = \Pr(\gamma_E < \zeta_E)$. Utilizing (3.34), and the expression $g = \ln \mu$, the outage probability can be written:

$$P_{oE} = \Pr\left(g < \ln \frac{\zeta_E}{M+1}\right). \tag{3.35}$$

Since g is normally distributed, (3.35) can be expressed

$$P_{oE} = 1 - \frac{1}{2}\mathrm{erfc}\left(\frac{\ln \frac{\zeta_E}{M+1} - m_g}{\sqrt{2}\,\sigma_g}\right), \tag{3.36}$$

where m_g and σ_g were previously defined in (3.22) and (3.23).

Eqs.(3.28) and (3.36) are expressions of the outage probability for two different criteria. When the communication link quality is sensitive to the instantaneous SIR, (3.28) should be used to evaluate the outage probability. Conversely, (3.36) is to be used when the average SIR determines the performance.

3.2.3 Probability of Bit Error

Average probability of bit error (P_e) is another important parameter to evaluate the performance of a wireless communications system. Computation of the bit error requires one to determine the distribution of the interference at array output. Due to dissimilar shadowing and fading effects, interferers are not identically distributed, hence the central limit theorem cannot be strictly invoked to claim the Gaussian property. Nevertheless, the Gaussian property is often assumed in such analyses [33, 36, 53, 54]. In this paper, the Gaussian assumption is validated by a chi-square test presented in Section 3.4

For BPSK and Gaussian interference, the bit error as conditional on the SIR is given by

$$P(e \mid \gamma) = \frac{1}{2}\mathrm{erfc}\left(\sqrt{\gamma/2}\right). \tag{3.37}$$

The density of γ conditioned on the input SIR μ is found from (3.11):

$$f(\gamma \mid \mu) = \frac{M(\gamma/\mu)^{M-1}}{\mu(1+\gamma/\mu)^{M+1}}. \tag{3.38}$$

The bit error averaged over $\gamma \mid \mu$ is given by:

$$\begin{aligned} P(e \mid \mu) &= \int_0^\infty P(e \mid \gamma) f(\gamma \mid \mu)\, d\gamma \\ &= \frac{1}{2} M \mu \int_0^\infty \operatorname{erfc}\left(\sqrt{\gamma/2}\right) \frac{\gamma^{M-1}}{(\mu+\gamma)^{M+1}} d\gamma. \end{aligned} \tag{3.39}$$

Following [55], (3.39) can be expressed utilizing hypergeometric functions as:

$$\begin{aligned} P(e \mid \mu) = \frac{M}{2\Gamma(M+1)} \Big[& \mu\, \Gamma(M+1)\, {}_2F_2\left(M+1, 1; \frac{3}{2}, 2; \frac{\mu}{2}\right) \\ & - \sqrt{2\mu}\, \Gamma\left(M+\frac{1}{2}\right) {}_2F_2\left(M+\frac{1}{2}, \frac{1}{2}; \frac{1}{2}, \frac{3}{2}; \frac{\mu}{2}\right) + \Gamma(M) \Big], \end{aligned} \tag{3.40}$$

where ${}_2F_2(\cdot)$ is generalized hypergeometric function, and is defined [56]:

$${}_pF_q(a_1, \cdots, a_p; , b_1, \cdots, b_q; x) = \sum_{n=0}^{\infty} \frac{(a_1)_n \cdots (a_p)_n}{(b_1)_n \cdots (b_q)_n} \frac{x^n}{n!}, \tag{3.41}$$

$(a)_n = \frac{\Gamma(a+n)}{\Gamma(a)}$, and $\Gamma(\cdot)$ is standard gamma function defined by:

$$\Gamma(z) = \int_0^\infty t^{z-1} e^{-t}\, dt, \quad (z > 0).$$

Eq.(3.40) can be evaluated by using software packages such as Maple, Mathematica, etc. Alternatively, (3.39) can be evaluated numerically.

The unconditional probability of bit error is found by averaging $P(e \mid \mu)$ over μ:

$$P_e = \int_0^\infty P_e(\mu) f(\mu) d\mu. \tag{3.42}$$

Replacing μ by e^g, one gets

$$P_e = \int_{-\infty}^{\infty} P_e(g) f(g) dg = E_g\left[P_e(g)\right], \tag{3.43}$$

where $P_e(g)$ is similar to (3.40), with μ replaced by e^g. Using an approach similar to the one used in the calculation of outage probability, the final expression of average probability of bit error can be written as:

$$\begin{aligned} P_e &= E_g\left[P_e(g)\right] \\ &\cong \frac{2}{3} P_e(m_g) + \frac{1}{6} P_e\left(m_g + \sqrt{3}\,\sigma_g\right) + \frac{1}{6} P_e\left(m_g - \sqrt{3}\,\sigma_g\right). \end{aligned} \tag{3.44}$$

3.3 Extensions of Previous Results

Some of the results developed up to now can be extended to more general cases. These include: other cell interference, correlation of shadowing among different users, channels with time dispersion, pilot tone effect, and system performance in terms of Erlang.

3.3.1 Other-Cell Interference

Since the reuse factor in CDMA systems is one, the users in neighboring cells also provide CCI. If the same loading is assumed in all cells, the effect of CCI introduced by users of all other cells is equivalent to the effect of CCI from qK_u users of the home cell [18]. With soft handoff, q lies between 0.5 and 0.6. Let $K_u' \triangleq K_u(1+q)$, then all the results developed so far apply with K_u replaced by K_u'.

3.3.2 Correlation of Shadowing Among Users

We assumed independent shadowing for different users in previous analyses, however the shadowings may be correlated in some practical situations even with individual power control when the received signals are shadowed by the same obstacles near the base station. In this case, a_k are not iid RVs. The correlation coefficient between a_k and a_j is defined by:

$$r_{kj} = \frac{E\left[(a_k - m_a)(a_j - m_a)\right]}{\sigma_a^2}, \tag{3.45}$$

where a_k and a_j are still assumed identically distributed with same mean and variance. For simplicity, we assume $r_{kj} = r$ for $k \neq j$ and $k, j = 1, \cdots, K_u'$. Eq. (3.17) is still valid, but (3.18) should be modified as:

$$p e^{2m_a + 2\sigma_a^2} \sum_{k=2}^{K_u'} \eta_k^2 + p^2 e^{2m_a} e^{\sigma_a^2(1+r)} \sum_{k=2}^{K_u'} \sum_{j \neq k} \eta_k \eta_j \equiv \epsilon^{\xi_2}, \tag{3.46}$$

and (3.23) becomes:

$$\sigma_g^2 = \sigma_a^2 + \sigma_b^2 - 2 r_{ab} \sigma_a \sigma_b, \tag{3.47}$$

where r_{ab} is the correlation coefficient between a_1 and b. The above results can be easily extended to the general case when r_{kj} are not equal, and a_k have different mean values and variances (see [28, 29] for more details about the expression of e^{ξ_2} and calculation of r_{ab}). All other results still hold.

3.3.3 Time Diversity

The reverse link channel is assumed frequency-selective with L resolvable paths. A RAKE receiver is used to track and combine the paths. The received signal of the lth path after spread spectrum demodulation can be expressed by the M-dimensional vector:

$$\begin{aligned} \mathbf{y}_l(i) &= \sqrt{\lambda_{1l}}\, s_1(i)\mathbf{c}_{1l} + \sum_{\substack{n=1 \\ n\neq l}}^{L} \sqrt{\lambda_{1n}} \left(s_1(i-1)\,\rho_{1ln}^{-} + s_1(i)\,\rho_{1ln}^{+} \right) \mathbf{c}_{1n} \\ &\quad + \sum_{k=2}^{K_u'} \sum_{n=1}^{L} \epsilon_k \sqrt{\lambda_{kn}} \left(s_k(i-1)\,\rho_{kln}^{-} + s_k(i)\,\rho_{kln}^{+} \right) \mathbf{c}_{kn}, \quad l = 1, \cdots, L, \end{aligned} \tag{3.48}$$

where $k = 1, \ldots, K_u'$ is the user index, $n = 1, \ldots, L$ is the path index, λ_{kn} are the received signal powers, $\mathbf{c}_{kn}$ are the channel vectors, τ_{kl} and τ_{kn} are the delays, and

$$\rho_{kln}^{-} = \int_{iT_s}^{iT_s+\tau_{kn}} u_k(t-\tau_{kn}) u_1(t-\tau_{1l})\,dt,$$

$$\rho_{kln}^{+} = \int_{iT_s+\tau_{kn}}^{(i+1)T_s} u_k(t-\tau_{kn}) u_1(t-\tau_{1l})\,dt.$$

Assume that all paths associated with a user have the same shadowing effect, that is $\lambda_{kl} = \lambda_k$, but are affected by independent Rayleigh fading. It is also assumed that the cross-correlations are independent of the path l, i.e., $\rho_{kln}^{-} = \rho_{kn}^{-}$ and $\rho_{kln}^{+} = \rho_{kn}^{+}$. Signal vectors associated with the different paths, $\mathbf{y}_l(i)$ $(l = 1, \cdots, L)$, are stacked to form an ML-dimensional vector, $\mathbf{y}(i)$, and grouped according to components related to the desired signal, interference and noise, yielding the expression (see [14] for details):

$$\mathbf{y}(i) = \sqrt{\lambda_1}\, s_1(i)\, \mathbf{c}_1 + \mathbf{i}(i), \tag{3.49}$$

where $\mathbf{y}(i) = \left[\mathbf{y}_1^T(i), \cdots, \mathbf{y}_L^T(i)\right]^T$, and $\mathbf{c}_1 = \left[\mathbf{c}_{11}^T, \cdots, \mathbf{c}_{1L}^T\right]^T$. The first term in the relation above represents the desired signal, $\mathbf{i}(i)$ is the interference, and the superscript "T" denotes transpose.

When MRC is used in both space domain (antenna array) and time domain (RAKE receiver), the output is the same as the output obtained by applying MRC to the stacked vector in (4.14). The MRC weight vector is given by $\mathbf{w} = \mathbf{c}_1$. Similar to the approach taken earlier, it is assumed that the interference can be expressed as an equivalent source:

$$\mathbf{i}(i) = s(i) \sum_{k=2}^{K_u} \sum_{n=1}^{L} \epsilon_k \sqrt{\eta_{kn}\lambda_{kn}}\ \mathbf{c}_{kn}, \tag{3.50}$$

where $s(i)$ is the CCI source bit, η_{kn} is a gain factor representing the cross-correlation between codes. The double sum over the ML-dimensional Gaussian distributed vectors $\mathbf{c}_{kn}$ is equivalent to another Gaussian vector,

$$\sum_{k=2}^{K_u} \sum_{n=1}^{L} \epsilon_k \sqrt{\eta_{kn}\lambda_{kn}}\ \mathbf{c}_{kn} = \sqrt{\mathcal{I}}\ \mathbf{c}_p,$$

where

$$\mathcal{I} = \sum_{k=2}^{K_u} \sum_{n=1}^{L} \epsilon_k \eta_{kn} \lambda_{kn} \tag{3.51}$$

$$= \sum_{k=2}^{K_u} \epsilon_k \nu_k \lambda_k, \tag{3.52}$$

where $\nu_k = \sum_{n=1}^{L} \eta_{kn}$. This form is similar to (3.13), therefore, (3.17) and (3.18) can be modified as:

$$\begin{aligned} E\left[\mathcal{I}'\right] &\cong E\left[\sum_{k=2}^{K_u'} \epsilon_k \nu_k e^{a_k}\right] \\ &= p\, e^{m_a + \sigma_a^2/2} \sum_{k=2}^{K_u'} \nu_k \ \equiv\ e^{\xi_1}, \end{aligned} \tag{3.53}$$

$$\begin{aligned} E\left[\mathcal{I}'^2\right] &\cong E\left[\left(\sum_{k=2}^{K_u'} \epsilon_k \nu_k e^{a_k}\right)^2\right] \\ &= p e^{2m_a + 2\sigma_a^2} \sum_{k=2}^{K_u'} \nu_k^2 + p^2 e^{2m_a} e^{\sigma_a^2(1+r)} \sum_{k=2}^{K_u'} \sum_{j \neq k} \nu_k \nu_j \ \equiv\ e^{\xi_2}, \end{aligned} \tag{3.54}$$

where the other-cell interference and the correlations of shadowings have been taken into account. Eqs.(3.19) and (3.20) are still valid while defining $b = \ln \mathcal{I}'$.

Since the space-time processing provides ML-branch diversity, the CDF and PDF of the output SIR (γ) conditioned on the input SIR, can be written as

$$F(\gamma \mid \mu) = \frac{(\gamma/\mu)^{ML}}{(1+\gamma/\mu)^{ML}}, \tag{3.55}$$

and

$$f(\gamma \mid \mu) = \frac{ML(\gamma/\mu)^{ML-1}}{\mu(1+\gamma/\mu)^{ML+1}}, \tag{3.56}$$

where $\mu = S/\mathcal{I}'$. All other results in Section 3.2 hold by using ML instead of M. Therefore, the effects of multipath and RAKE receiver result are the gain of degree of diversity and the increase of total interference power.

3.3.4 Pilot-Aided Coherent Detection

Pilot-aided coherent detection and perfect channel estimation in reverse link are assumed. The power-split ratio for the pilot is r_p, then the fraction of the total transmitted power used for information traffic is $1/(1+r_p)$. With this model, the instantaneous output SIR is given by $\gamma' = \kappa\gamma$, where $\kappa = 1/(1+r_p)$, and γ was given in (3.10). Therefore the CDF and PDF of γ' can be modified from (3.55) and (3.56):

$$F(\gamma' \mid \mu) = \frac{(\gamma'/\kappa\mu)^{ML}}{(1+\gamma'/\kappa\mu)^{ML}}, \tag{3.57}$$

$$f(\gamma' \mid \mu) = \frac{ML(\gamma'/\kappa\mu)^{ML-1}}{\kappa\mu(1+\gamma'/\kappa\mu)^{ML+1}}. \tag{3.58}$$

Other results, $P_o(g)$ and $P_e(g)$, can be modified accordingly. Especially, for average SIR outage, the average signal power at the array output is given by

$$S' = \kappa S,$$

and the average SIR is written as

$$\gamma'_E = (M+1)\kappa\mu.$$

Finally (3.36) can be modified as

$$P_{oE} = 1 - \frac{1}{2}\mathrm{erfc}\left(\frac{\ln\frac{\zeta_E}{\kappa(ML+1)} - m_g}{\sqrt{2}\,\sigma_g}\right). \tag{3.59}$$

3.3.5 Performance in Terms of Erlang Capacity

For a communication system, another capacity measurement is in terms of Erlangs per cell. In slotted communication systems (frequency-division and time-division multiple access), blocking probability is used in the Erlang capacity analysis. For nonslotted CDMA system, Erlang capacity is determined by the outage probability. In this case, the number of active users in the system is a random variable, which follows Poisson distribution [18]:

$$P[K_u = k] = \frac{\beta^k}{k!}\, e^{-\beta}, \qquad k = 0, 1, 2, \cdots \tag{3.60}$$

where the parameter β is related to the call arrival rate and call service rate. The parameter β is amended to $\beta(1+q)$ for K_u', if we take into account the other cell interference. For a Poisson RV, the mean value and variance of K_u' are given by

$$E[K_u'] = Var[K_u'] = \beta(1+q).$$

Utilizing this model, the first and second moment of $\mathcal{I}'$ in (3.53) and (3.54) should be averaged over ϵ_k, a_k and K_u'. For brevity, we assume $\nu_k = \nu$. Then (3.53) and (3.54) can be modified as:

$$\begin{aligned} E[\mathcal{I}'] &\cong E_{K_u'}\left\{E_{\epsilon_k, a_k}\left[\sum_{k=2}^{K_u'} \epsilon_k \nu_k e^{a_k}\right]\right\} \\ &= \left[\beta(1+q) - 1\right] p\nu\, e^{m_a + \sigma_a^2/2} \\ &\equiv e^{\xi_1}, \end{aligned} \tag{3.61}$$

$$
\begin{aligned}
E\left[\mathcal{I}'^2\right] &\cong E_{K_u'}\left\{E_{c_k,a_k}\left[\left(\sum_{k=2}^{K_u'} c_k \nu_k e^{a_k}\right)^2\right]\right\} \\
&= p\nu^2 e^{2m_a+2\sigma_a^2}\left[\beta(1+q)-1\right] \\
&\quad + p^2\nu^2 e^{2m_a} e^{\sigma_a^2(1+r)}\left[\beta^2(1+q)^2 - 2\beta(1+q)+2\right] \\
&\equiv e^{\xi_2}. \qquad (3.62)
\end{aligned}
$$

By using (3.61) and (3.62) instead of (3.53) and (3.54), the outage probability of both instantaneous SIR and average SIR can be expressed in terms of Erlangs per cell (β).

3.4 Numerical Results

Numerical results in this section are generated from computer simulations of a cellular CDMA system employing BPSK modulation and BPSK spreading, with a voice activity factor of $p = 3/8$ and a spreading ratio of 156. The spreading ratio corresponds to a bandwidth of 1.25 MHz and an information bandwidth of 8 kHz. The channel was assumed flat and subject to Rayleigh fading.

First, the goodness of the Gaussian approximation was evaluated with the number of multiple paths $L = 1$. The number of antenna elements assumed was $M = 4$, the number of users $K_u = 30$, and PCE = 1.5 dB. To that end, the histogram of the interference was generated and compared to the a theoretical Gaussian curve. This is shown in Figure 3.2. Additionally, a chi-square test was applied (see [18] for details) to determine the goodness of fit of a Gaussian distribution to the computer generated data of interference. The sample space was partitioned into 21 disjoint intervals, and the chi-square statistic D^2 had a pdf that was approximately a chi-square pdf with 20 degrees of freedom. Standard chi-square test tables show that for 20 degrees of freedom, the threshold for a 1% significance level is 37.57. Calculated from the simulation and averaged over 200 Monte Carlo runs, the chi-square statistic

D^2 is 22.14, which does not exceed the threshold. From both the Gaussian cerve fitting and the chi-sqaure test, it can be concluded that the Gaussian approximation is valid for the interference.

The outage probability with respect to the instantaneous SIR is plotted in Figure 3.3 as a function of the capacity (number of users/cell) with the PCE as a parameter. The outage threshold is set at $\zeta = 7$ dB. Analytical curves are calculated from (3.28). Simulation curves are averages compiled from one million samples. For an outage probability of 10^{-2}, the system capacity is approximately 38, 32, 22, and 10 users/cell for PCE = 0, 1.5, 2.5 and 4.0 dB, respectively. In a CDMA system with PCE 1.5 to 2.5 dB, the system capacity degrades by 16% to 42% as compared to the case of perfect power control. Figure 3.3 shows a good match between analytical results and simulations.

To see the effect of PCE on the system capacity clearly, Figure 3.4 shows the capacity versus PCE, for an outage of 1%. The parameters used in this figure is the same as in Figure 3.3. This result demonstrates that the relation between the system capacity and PCE is nonlinear. In the range of PCE = 1 to 4 dB, the capacity decreases almost linearly at the rate of about 8 users/cell/dB. When the PCE increases to 6 dB, the system capacity is below 5 users/cell.

The effect of space diversity (analytical results only) is shown in Figure 3.5, for PCE = 1.5 dB, $M = 1$ to 8, and all other parameters are similar to those used in Figure 3.3. With $P_o = 10^{-2}$, 8-branch space diversity provides a capacity of 87 users/cell, while the capacity for two-branch space diversity is only 9 users/cell. Without space diversity ($M = 1$), the system capacity is below 5 users/cell. Utilizing the results in Figure 3.5, and setting $P_o = 10^{-2}$, Figure 3.6 shows that the capacity increases almost linearly with the degrees of space diversity; the capacity increase for each additional degree of space diversity is approximately 13 users/cell.

Now, we examine the outage probability of average SIR. The outage threshold is set at $\zeta_E = 7$ dB. The analytical curves in Figure 3.7 are computed from (3.36), and the simulation curves are based on ten million samples. For an outage of 10^{-2}, the system capacity is approximately 357, 170, 90 and 30 users/cell for PCE = 0, 1.5, 2.5 and 4.0 dB, respectively. Consequently, for PCE = 1.5 to 2.5 dB, the system capacity degrades by 52% to 75% as compared to the case of perfect power control. Comparing Figures 3.3 and 3.7, we conclude that for same threshold, the system capacity is much larger for an outage computed from the average SIR than for the computation based on the instantaneous SIR. However, the average SIR outage degrades faster due to PCE. The effect of space diversity on the outage probability for average SIR is shown in Figure 3.8 for parameters similar to those used in Figure 3.5. For $P_o = 10^{-2}$, the system capacity is about 31 to 276 users/cell for $M = 1$ to 8, i.e., the average capacity increase for each additional degree of space diversity is about 34 users/cell. To see clearly the effects of PCE and antenna arrays, Figure 3.9 gives the analytical results of capacity change with the PCE and number of antenna elements for $P_{oE}(\gamma_E < 7\text{dB}) = 0.01$. The figure shows that for capacity 60 users/cell, single-element receiver at base station requires less 1.7 dB PCE, while eight-element receiver can relief this requirement to 3.8 dB. For certain system PCE, the capacity can be found for different number of antenna elements. For example, when PCE = 2.5 dB, the system capacity is 35 users/cell to 165 users/cell for $M = 1$ to 8, respectively. This figure can be easily used to estimate the system capacity when the system configuration and power control capability are known.

For the probability of bit error, Figure 3.10 displays both the simulation and analytical results for the probability of bit error as a function of the number of users per cell. The simulation results are obtained using 200,000 samples per data point. The system capacity is the same as in Figure 3.3. If the desired performance is $P_e = 10^{-3}$, the capacity is respectively 51, 42, 30 and 15 users/cell for PCE = 0, 1.5,

2.5 and 4.0 dB. In a CDMA system with PCE 1.5 to 2.5 dB, the system capacity degrades by 18% to 41% as compared to the case of perfect power control. Figure 3.11 gives the analytical curves for PCE = 1.5 dB, $M = 1$ to 8. For $P_e = 10^{-3}$, the capacity is about 11 to 110 users/cell, respectively.

Next, we examine the extended results in Section 3.4. It is assumed that $M = 4$, $L = 4$ and $r = 0$, all other parameters are the same as in Figure 3.7. Figure 3.12 shows the outage probability for average SIR. For $P_o = 10^{-2}$, Figure 3.12 shows that the system capacity K'_u is 300, 145, 76 and 25 users for PCE = 0, 1.5, 2.5 and 4.0 dB, respectively. Figure 3.13 also gives the curves for PCE = 1.5 dB, and $M = 1$ to 8.

The effect of correlation between the shadowings is also examined. Figure 3.14 shows the curves for PCE = 1.5 dB, $M = 4$, $L = 4$ and different values of correlation coefficient (r). For $r = 0.2$ to 1, the system capacity degrades by 6% to 23% as compared to the uncorrelated shadowing case ($r = 0$).

In the interest of Erlang capacity, Figure 3.15 depicts the analytical curves of outage probability for average SIR versus $\beta(1 + q)$, where $M = 4$, $L = 1$, $r = 0$, $p = 3/8$, and PCE = 0, 1.5, 2.5, and 4.0 dB, respectively. Pilot tone effect is not included. This figure is similar to Figure 3.7, and gives an alternative to show the performance when considering the Erlang capacity.

3.5 Summary

In this chapter, we have studied the reverse link performance of cellular CDMA systems, which included the effects of space-time processing, Rayleigh fading, power control error and voice activity factor. The performance was analyzed in terms of outage probability for instantaneous output SIR and average output SIR, as well as average probability of bit error. The analytical results gave the simple, but accurate approximations to the system performance, and all the parameters needed in calculation could be measured from the data. The results were also extended

to more general cases, which include other cell interference, correlation between the shadowing, pilot tone effect and performance in terms of Erlang capacity. The analysis showed that space-time processing, which was provided by cell site antenna arrays along with RAKE receivers, improved the system performance and capacity, and compensated the performance loss due to power control error in cellular CDMA systems. Computer simulations showed a good match to the analytical expressions developed in the context.

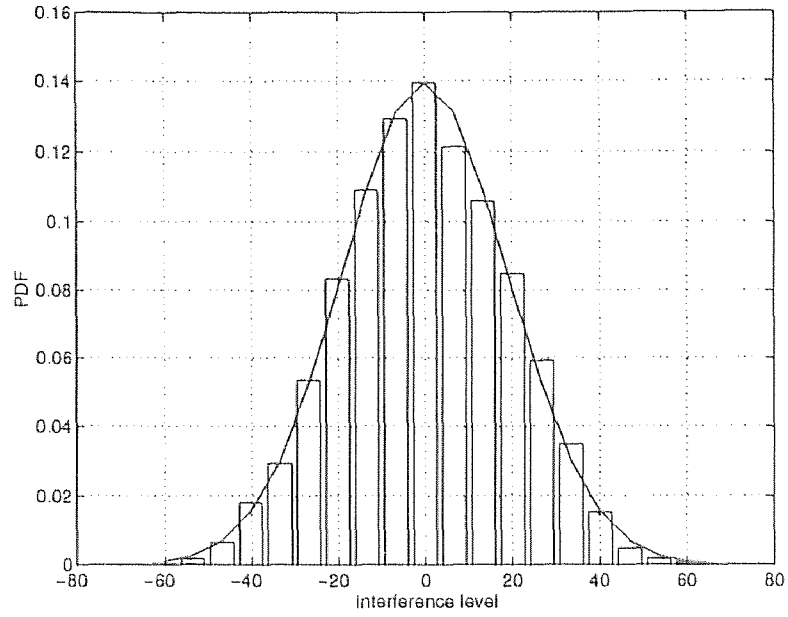

Figure 3.2 Interference distribution

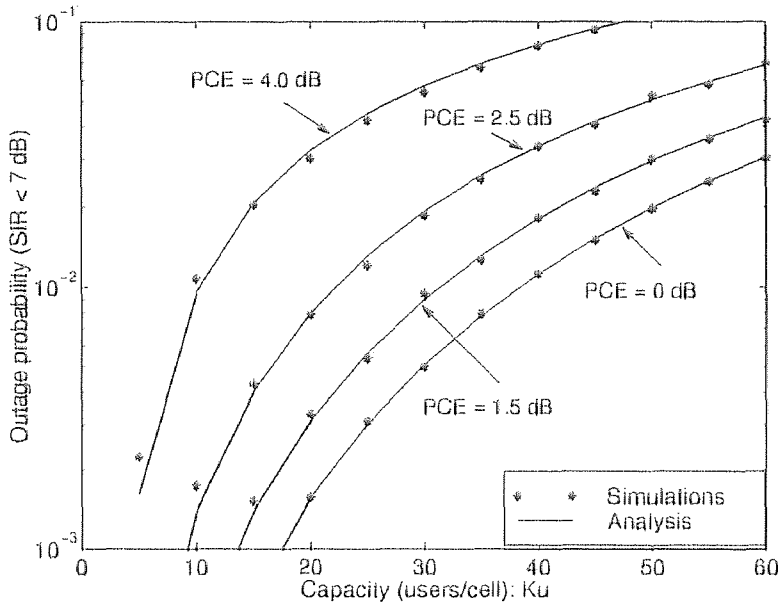

Figure 3.3 Outage probability versus capacity. Four antenna elements ($M = 4$), different PCEs, and $p = 3/8$.

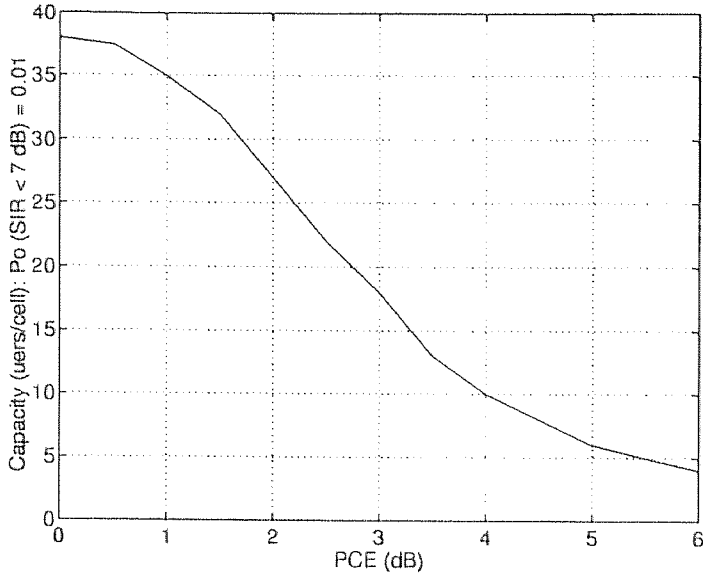

Figure 3.4 Capacity (users/cell) versus PCE. Analytical results for $M = 4$, $p = 3/8$ and $P_o(\gamma < 7 \text{ dB}) = 10^{-2}$.

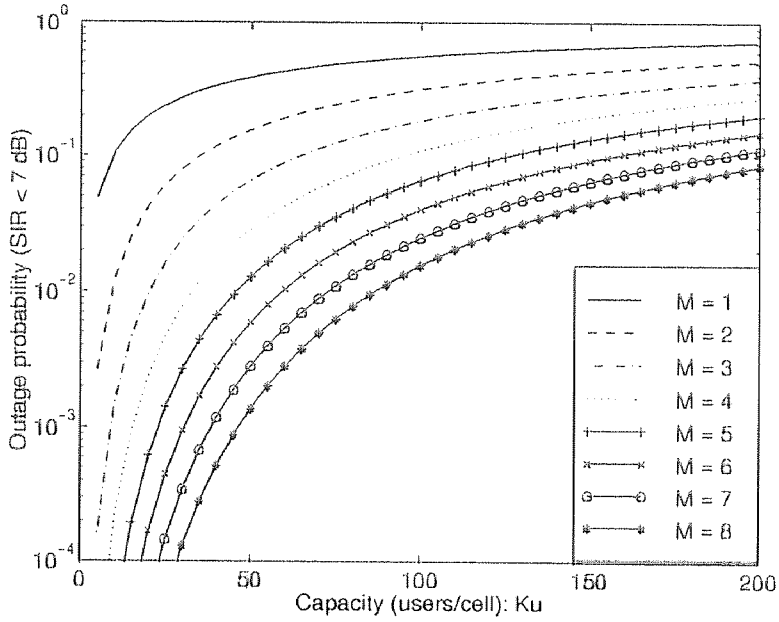

Figure 3.5 Outage probability versus capacity. Analytical results for PCE = 1.5 dB, $M = 1$ to 8, and $p = 3/8$.

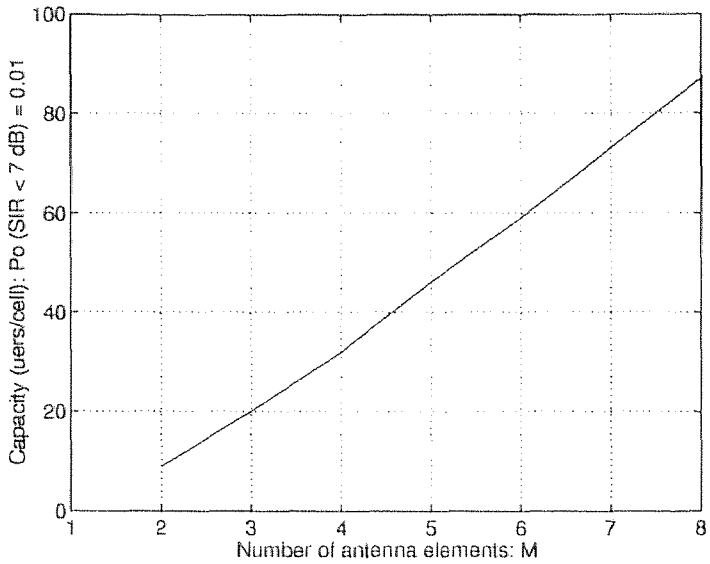

Figure 3.6 Capacity (users/cell) versus number of antenna elements. Analytical results for PCE = 1.5 dB, $p = 3/8$ and $P_o(\gamma < 7\ \text{dB}) = 10^{-2}$.

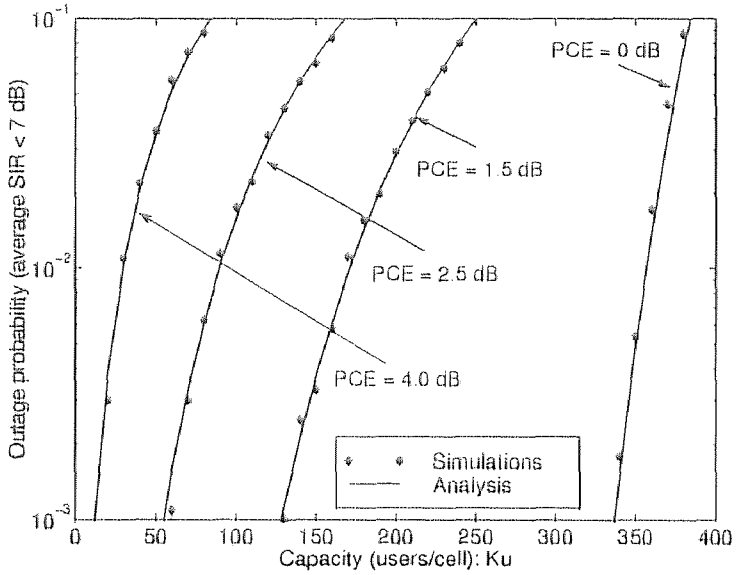

Figure 3.7 Outage probability versus capacity (users/cell), consider the average SIR. Four antenna elements ($M = 4$), different PCEs, and $p = 3/8$.

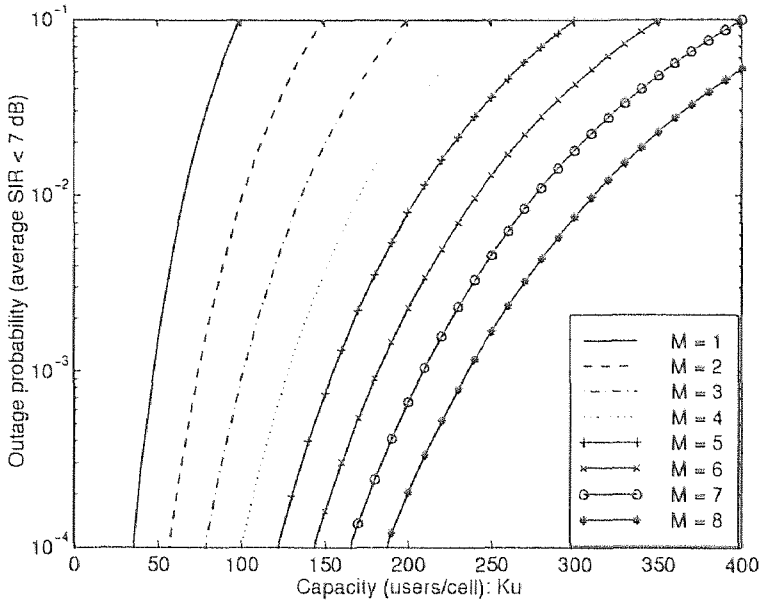

Figure 3.8 Outage probability versus capacity (users/cell), consider the avearge SIR. Analytical results for PCE = 1.5 dB, $M = 1$ to 8, and $p = 3/8$.

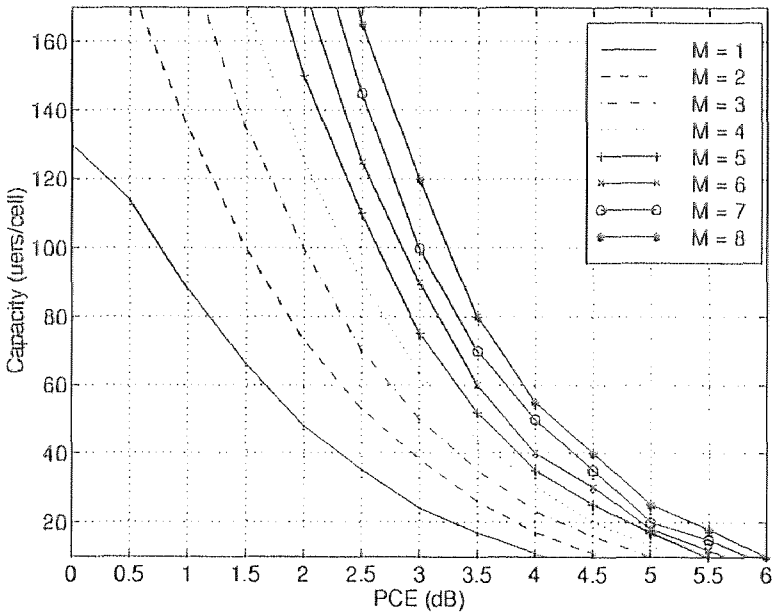

Figure 3.9 Capacity (users/cell) versus PCE for $P_{oE}(\gamma_E < 7 \text{ dB}) = 0.01$. Analytical results for $M = 1$ to 8, and $p = 3/8$.

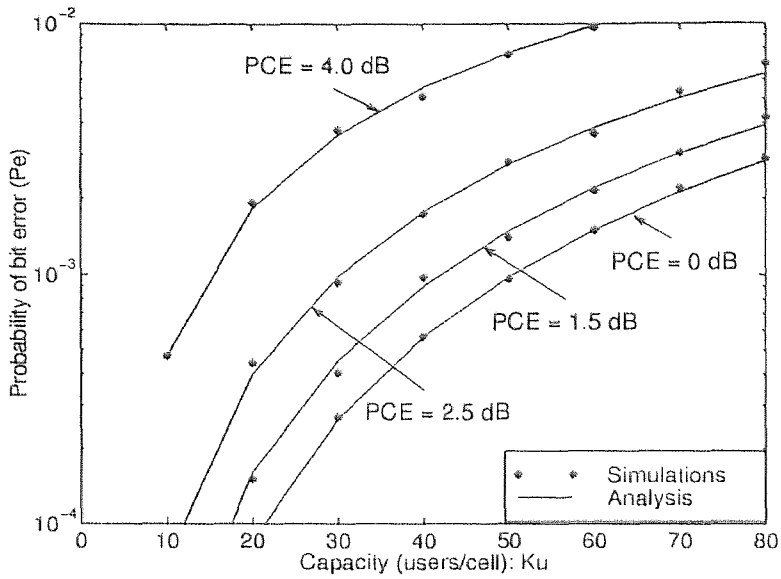

Figure 3.10 Probability of bit error versus capacity (users/cell). Four antenna elements ($M = 4$), different PCEs, and $p = 3/8$.

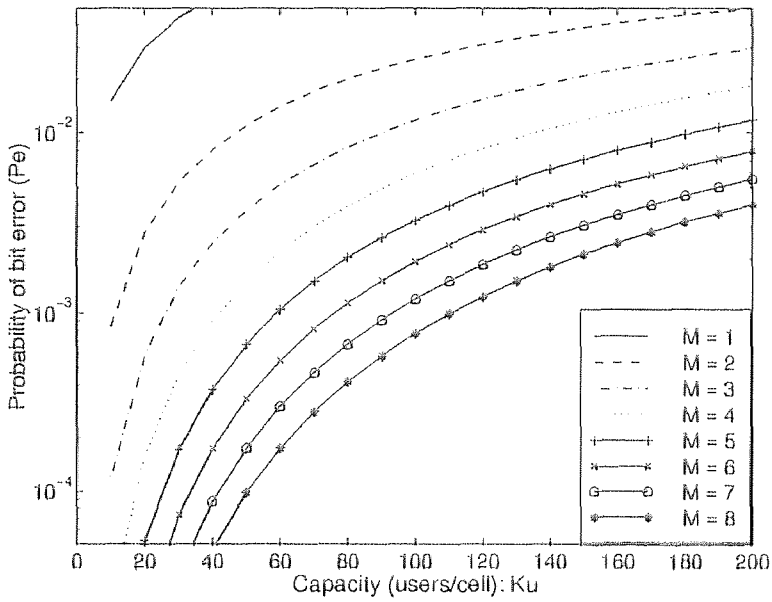

Figure 3.11 Probability of bit error versus capacity (users/cell). Analytical results for PCE = 1.5 dB, $M = 1$ to 8, and $p = 3/8$.

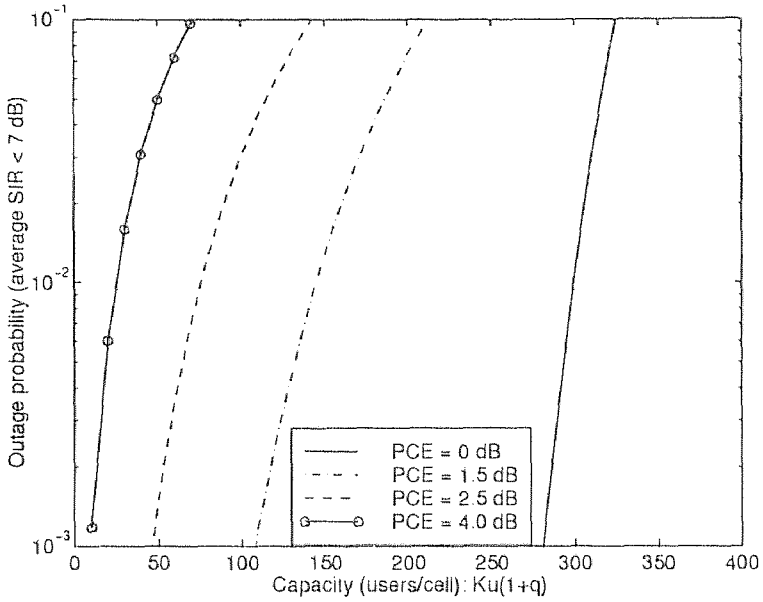

Figure 3.12 Outage probability versus capacity (users/cell), consider the avearge SIR. Four antenna elements ($M = 4$), four resolvable paths ($L = 4$), $r = 0$, different PCEs, and $p = 3/8$.

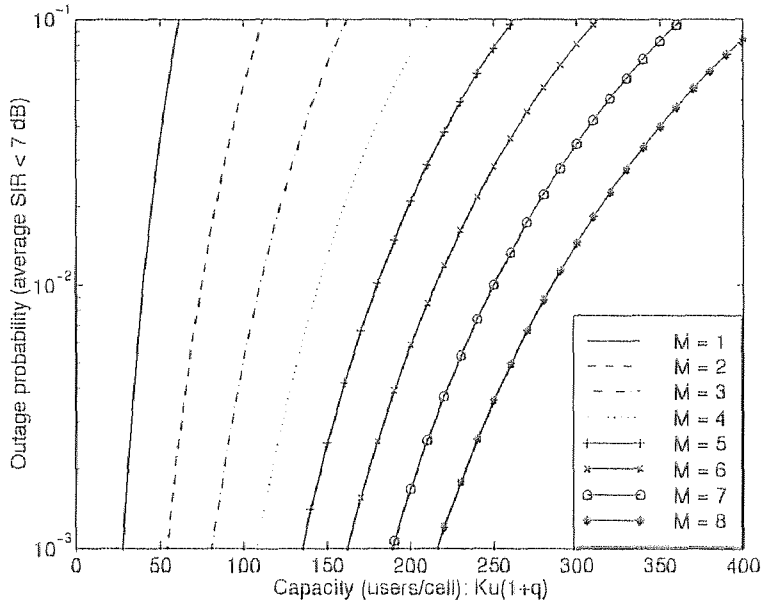

Figure 3.13 Outage probability versus capacity (users/cell), consider the avearge SIR. Analytical results for PCE = 1.5 dB, four resolvable paths ($L = 4$), $r = 0$, $M = 1$ to 8, and $p = 3/8$.

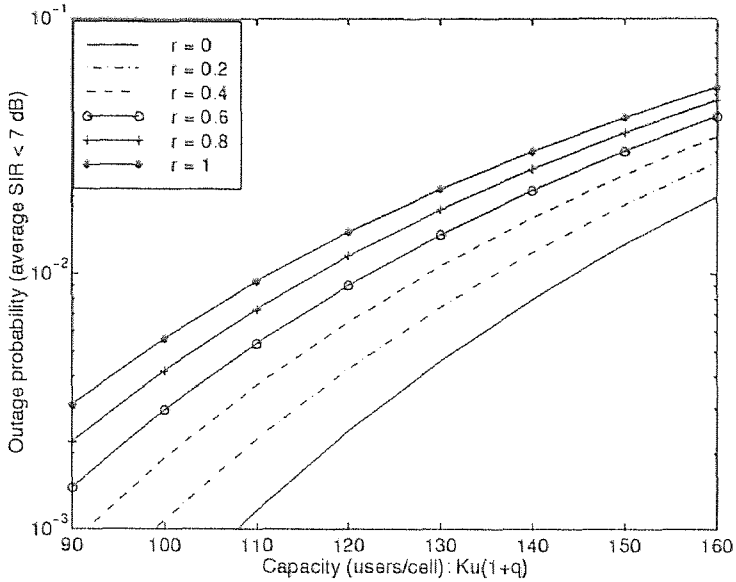

Figure 3.14 Outage probability versus capacity (users/cell), consider the avearge SIR. Four antenna elements ($M = 4$), four resolvable paths ($L = 4$), PCE = 1.5 dB, different values of correlation efficient (r), and $p = 3/8$.

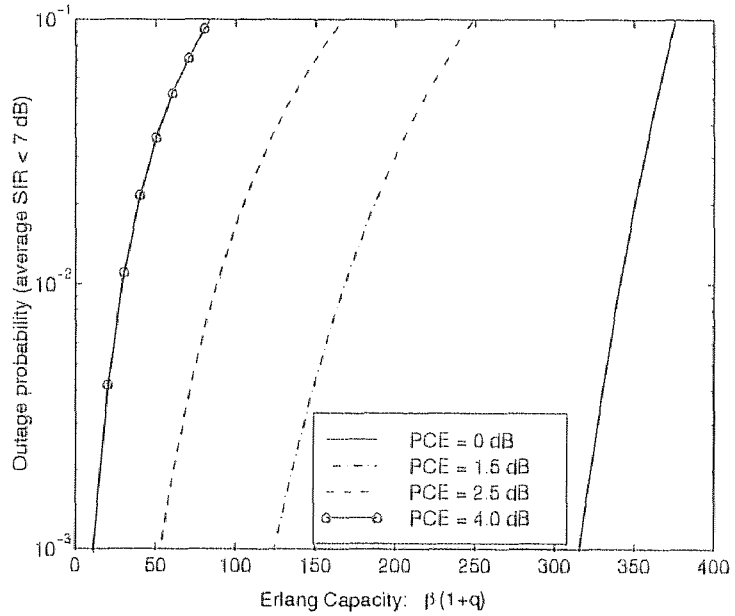

Figure 3.15 Outage probability versus Erlang capacity, consider the avearge SIR. Four antenna elements ($M = 4$), one resolvable path ($L = 1$), $r = 0$, different PCEs, and $p = 3/8$.

CHAPTER 4

APPLICATION OF ADAPTIVE ANTENNA ARRAY IN CDMA FORWARD LINK RECEIVER

This chapter explores the application of an antenna array in the forward link receiver of a CDMA communications system. While the accurate synchronization and orthogonality of Walsh codes in forward link can minimize intra-cell interference, asynchronous signals from neighboring base stations cause inter-cell interference. In fact, the intra-cell interference cannot be eliminated since multipath fading creats self interference. Figure 4.1 shows the cellular structure for wireless CDMA communications. At the cell boundary point p, the mobile station (communicating with base station B_0) may confront strong interference from base stations B_2 and B_3 while the desired signal from home base station B_0 is weaker, causing the communication performance to degrade.

An adaptive antenna array, which is referred to as a smart antenna, is proposed at the mobile station for interference suppression; the performance improvement due to such an antenna array is analyzed and demonstrated by numerical simulations. Since the proposed wireless CDMA systems, like J-STD-008 (PCS) and J-STD-015 (Wideband CDMA) are all based on IS-95A, in the context, IS-95A CDMA will be used as an example to illustrate the implementation of the proposed smart antenna.

4.1 CDMA Forward Link Spreading Logic

To design the adaptive antenna array used at the mobile station, first, it is useful to describe the forward link signal structure transmitted by the base station. In IS-95A CDMA, all base stations radiate a universal code which is searched by the mobile stations. All base stations are synchronized to a universal system time by global positioning system (GPS), then phases of the universal codes can be coordinated.

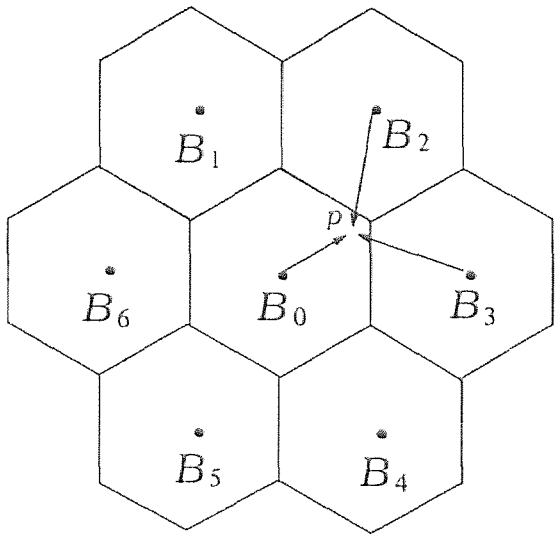

Figure 4.1 Cellular structure for wireless CDMA communications.

In particular, base stations are assigned different phases in order to make them distinguishable by the mobile stations.

The minimum separation of code phases is related to the largest cells present in a system. The separation must be larger than the propagation delay that can be incurred by a usable base station. The air interface standards call out a separation increment of 64 chips (about 15.6 km of one-way propagation delay) between base stations.

The universal code, which is also referred to as *short code*, has a period of 2^{15}, which is 27.667 ms at the 1.2288 MHz spreading rate. The short code is composed of two different sequences, one for the I-channel and another for the Q-channel. They have different generators and low cross-correlation. The short code is generated from a period $2^{15} - 1$ linear feedback shift register (LFSR) sequence, and an extra zero bit is added to bring the length to an even power of two.

The maximum-length shift-register (MLSR) sequences produced by LFSRs are widely used to generate pseudo-noise (PN) sequence for direct sequence spectrum spreading. An m-bit MLSR produces a sequence of period $2^m - 1$. If the sequence is

mapped to a binary valued waveform by mapping a binary zero to -1 and binary 1 to $+1$, then the auto-correlation is unity for zero delay, and $-1/(2^m - 1)$ at all other delays [17, 18].

The short code LFSR tap polynomials are [20, p.527], for the I-sequence

$$P_I(X) = X^{15} + X^{13} + X^9 + X^8 + X^7 + X^5 + 1, \tag{4.1}$$

and for the Q-sequence

$$P_Q(X) = X^{15} + X^{12} + X^{11} + X^{10} + X^6 + X^5 + X^4 + X^3 + 1. \tag{4.2}$$

The extra zero bit is inserted in each sequence immediately after the occurence of 14 consecutive zeros from the generator register. This occurs once per period.

Because each base station must serve many users at the same time, there must be some way of creating independent communication channels. Moreover, because these channels all come from the same base station, they can share precise timing, and must somehow share the common PN short code spreading. Each forward link traffic channel is spread with a Walsh function, which consists of 64 binary sequences. These sequences have the property that the "dot product" of any two of them is zero. The Walsh function of order 4, for example, is:

$$\mathbf{W}_4 = \begin{bmatrix} + & + & + & + \\ + & - & + & - \\ + & + & - & - \\ + & - & - & + \end{bmatrix}. \tag{4.3}$$

From the nth order Walsh function $\mathbf{W}_n$, one can generate the $2n$th order Walsh function $\mathbf{W}_{2n}$ according to the relation [17]:

$$\mathbf{W}_{2n} = \begin{bmatrix} \mathbf{W}_n & \mathbf{W}_n \\ \mathbf{W}_n & \overline{\mathbf{W}}_n \end{bmatrix}, \tag{4.4}$$

where $\overline{\mathbf{W}}_n$ denotes the complement of $\mathbf{W}_n$.

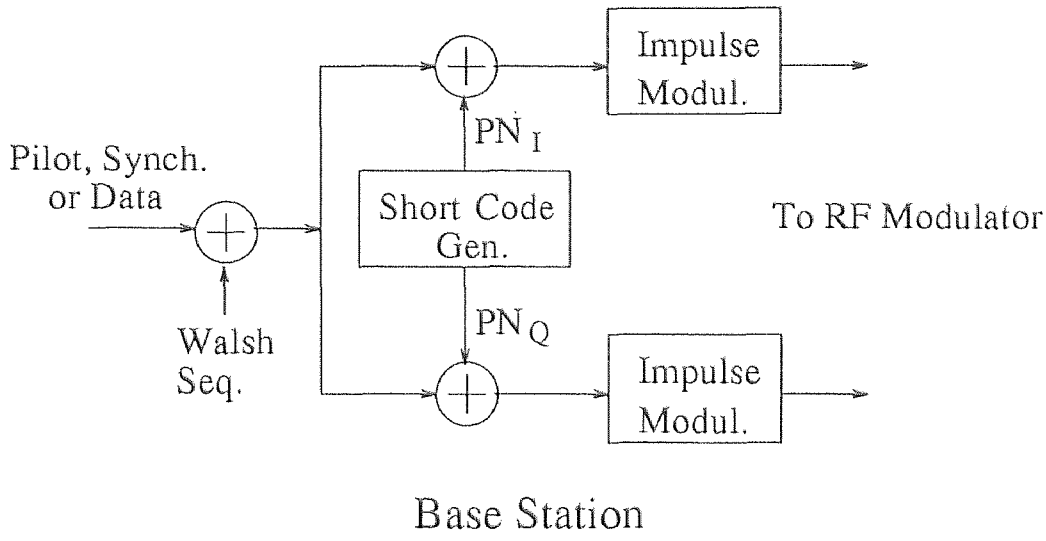

Figure 4.2 CDMA forward link spreading logic.

Walsh function of order 64 is used in the forward CDMA channel to create 64 orthogonal channels. There is exactly one period of the Walsh sequence per code symbol. These channels are readily generated by the binary logic shown in Figure 4.2. The "impulse modulators" generate a discrete ± 1 outputs in response to binary (0,1) inputs. Summing the code symbols, the Walsh cover, and the two PN short code sequences, and changing to the bipolar ± 1 representation, result in a quadrature (I,Q) sequence of elements. These elements drive a modulator that generates the appropriately bandlimited analog output.

One of the Walsh sequences, numbered zero, has all 64 chips the same. By the logic of Figure 4.2, this is just the "bare" PN short code spreading. It is the universal *pilot* sequence that all mobile stations use as their search target.

4.2 System Model

Based on the forward link signal structure, a small antenna array with two elements is considered at a mobile station of a cellular CDMA system. Assume that there are one home base station ($j = 0$), and J neighboring base stations, where the jth ($j =$

$0, 1, \cdots, J$) base station serves $K_j + 1$ active users. The signal from each base station is composed of $K_j + 1$ users' information waveforms and one pilot waveform. The signals from different base stations are assumed to independently undergo Rayleigh fading, while the $K_j + 2$ waveforms that arrive from the same base station at a given mobile station propagate over the same path. In this section, a single path is assumed, and the multipath case will be discussed in Section 4.5. With the above model, the complex envelope of the received signal at two antenna elements of the mobile station is given by a 2×1 vector:

$$\mathbf{r}(t) = \sum_{j=0}^{J} \mathbf{c}_j(t) \left\{ \sum_{k=0}^{K_j} \sqrt{P_{ju}} \cdot d_{jk}(t - \tau_j) \cdot u_{jk}(t - \tau_j) + \sqrt{P_{jp}} \cdot u_j(t - \tau_j) \right\} + \mathbf{v}(t), \tag{4.5}$$

where $\mathbf{c}_j(t)$ are 2×1 vectors representing complex Gaussian channels, $d_{jk}(t)$ are transmitted information symbols, P_{ju} and P_{jp} are the unfaded received powers of the users' and the pilot signals respectively, $u_j(t)$ are the PN short codes, and $\mathbf{v}(t)$ is a 2×1 vector representing AWGN. Since symbol timing of all base stations are synchronized with a GPS signal, as reference to this time, τ_j is the propagation delay from the jth base station, $u_{jk}(t) = W_{jk}(t) \cdot u_j(t)$ with $W_{jk}(t)$ the Walsh sequence of user k and base station j. Also $u_j(t) = u(t - \tau_j')$, where $u(t)$ is the short code with zero shift and τ_j' the shift of the short code of the corresponding base station. The following assumptions are adopted in the analysis:

- intra-cell interference is eliminated due to the orthogonality among u_{jk} for users in same cell.
- communication performance is examined for user 0 in cell 0, for which the channel vector can be written as: $\mathbf{c}_0 = [c_{01}, c_{02}]^T$.
- without loss of generality, set $\tau_0 = \tau_0' = 0$.

A generalized sidelobe canceller (GSC) with a small antenna array (two elements) can be applied for spread spectrum communications, and its operation

can be explained by referring to Figure 4.3. The complex parameter s_1 is the beam steering weight which, when properly set, generates an amplitude equal and phase coherent signals at two inputs of the hybrid. The hybrid which generates the sum (y_b) and the difference (z) signals eliminates the desired signal at point z. The weight s_2 is used for estimating the interference, which is substracted from y_b, so that higher SINR can be obtained at the array output y and the despread output d_o. The weight s_2 can be updated by several methods, such as least mean square (LMS), recursive least square (RLS), or direct matrix inversion (DMI). When the channel vector estimate is erroneous, s_1 will not result in null difference between the desired signals received at two antennas, the residual desired signal contributions at z will be interpreted by the array as interference, and hence cancelled. This results in performance degradation of the canceller [41, 42].

4.3 Adaptive Correction

In Figure 4.4, an adaptive loop is proposed for self-correcting the beam steering weight s_1. Using the home base station PN short code $u(t)$, the processor at the mobile station despreads the array output of ith symbol interval $y(i,t)$ ($t = iT_s \sim (i+1)T_s$), averages over time T_s, then respreads with the same on-time code to get a reference signal $g(i,t)$, where T_s denotes symbol interval. The control signal $h_1(i)$ is generated by accumulating the output of multiplying of $g(i,t)$ and $z(i,t)$ over one symbol interval, while $h_2(i)$ is generated by accumulating the output of multiplying of $g(i,t)$ and $r_1(i,t)$ over the same symbol interval. Both signals $h_1(i)$ and $h_2(i)$ are used to correct the beam steering weight s_1. The algorithm for adaptive correction of s_1 is formulated as follows:

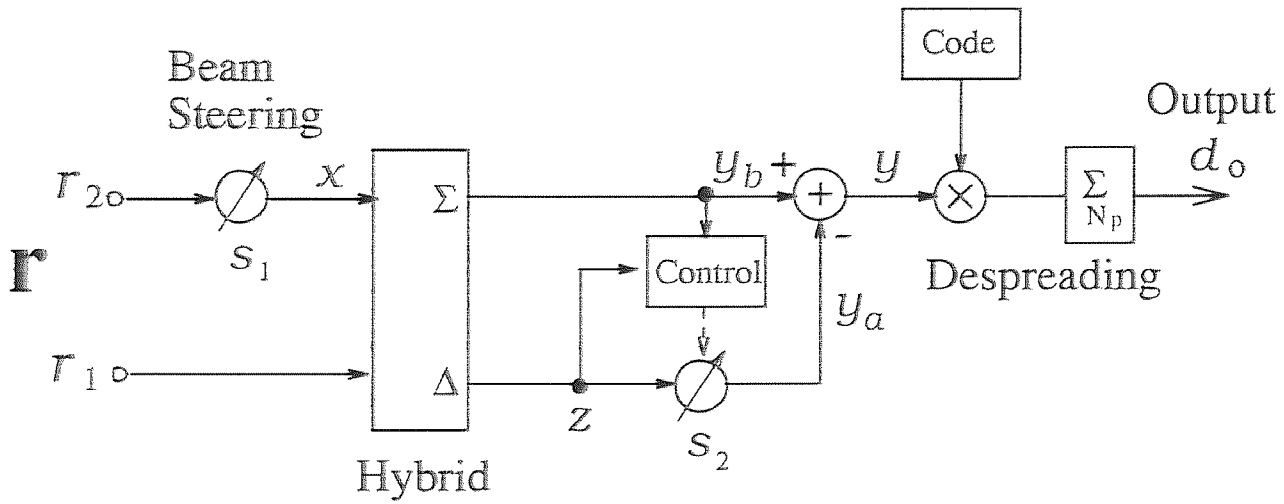

Figure 4.3 Interference canceller for spread spectrum communications.

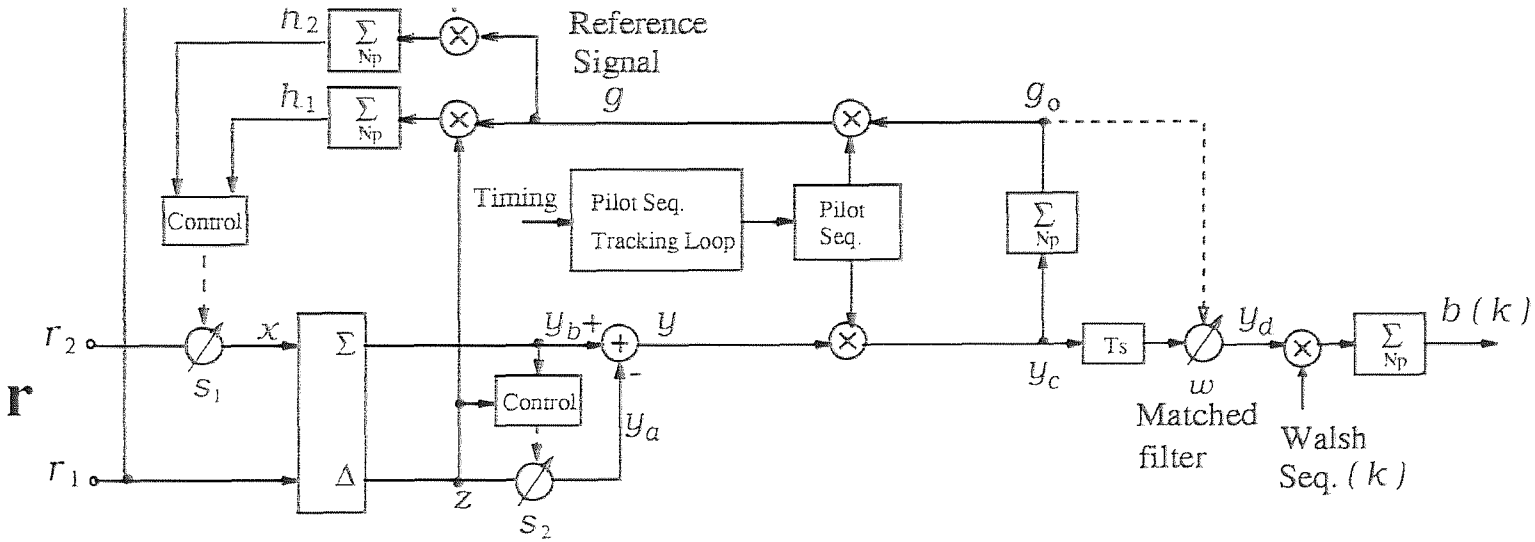

Figure 4.4 Smart antenna at the mobile station for wireless CDMA communications.

Algorithm:

1. Initialization: $s_1(0)$ can be chosen according to prior desired signal channel estimation, or simply set $s_1(0) = 1$.

2. For symbol interval $i = 0, 1, \cdots$

   $x(i,n) = s(i)\, r_2(i,n)$, where n denotes nth chip in ith symbol.

3. $z(i,n) = r_1(i,n) - x(i,n)$.

4. $y_b(i,n) = r_1(i,n) + x(i,n)$.

5. $y_a(i,n) = z(i,n)\, s_2(i)$,

   where the weight $s_2(i)$ can be computed, for example, by DMI. Since $s_2(i)$ is a scalar, the correlation matrix and cross-correlation vector for the DMI become scalars. By DMI, $s_2(i) = [R_z^{-1}(i)\, f_{z,y_b}(i)]^*$, where $R_z(i) = \frac{1}{N_p}\sum_{N_p} z(i,n)\, z^*(i,n)$, $f_{z,y_b}(i) = \frac{1}{N_p}\sum_{N_p} z(i,n) y_b^*(i,n)$, and the superscript "$*$" denotes complex conjugate, and N_p is the number of code chips per symbol.

6. The array output: $y(i,n) = y_b(i,n) - y_a(i,n)$.

7. Despreading: $g_o(i) = \frac{1}{N_p}\sum_{n=1}^{N_p} y(i,n) u_{0p}(i,n)$.

8. Respreading: $g(i,n) = g_o(i) u_{0p}(i,n)$.

9. $h_1(i) = \frac{1}{N_p}\sum_{n=1}^{N_p} z(i,n)\, g^*(i,n)$.

10. $h_2(i) = \frac{1}{N_p}\sum_{n=1}^{N_p} r_1(i,n)\, g^*(i,n)$.

11. The estimated weight s_1 can be calculated through the recursion:

$$\hat{s}_1(i) = s(i) + \frac{h_1(i)}{h_2(i) - h_1(i)} \cdot s_1(i), \tag{4.6}$$

    which is used to process the signal of the ith symbol interval.

12. The $\hat{s}_1(i)$ is used as the initial weight for next time interval:

$$s_1(i+1) = \hat{s}_1(i). \tag{4.7}$$

The value of $h_1(i)$ depends on the beam steering weight error and the signal power from the home base station. Therefore, $h_2(i)$ is used to estimate the signal power from home base station, such that the self-correcting loop can extract the information only related to the beam steering weight error in step 11. Note that only if the weight s_1 is properly set, and $z(i,n)$ contains no signal from the home base station, the reference signal $g(i,n)$ is uncorrelated with $z(i,n)$, $h_1(i)$ will be zero and the beam steering weight s_1 keeps unchange, which is the desired result. It can be shown that this algorithm gives an estimate of the channel vector error between two antenna elements, and the weight $s_1 = c_{01}/c_{02}$ when pure reference signal is available at g. Since y is with higher SINR than the array input, the matched filter w (matched to the channel attenuation and phase delay) operated from y is more accurate than the one estimated from single antenna input r_1:

$$w = \frac{1}{\sqrt{E_c}\, N_p} \sum_{n=1}^{N_p} y(i,n) a_{0p}(i,n),$$

where E_c denotes the energy per chip. The array output y is despread by pilot and kth user's Walsh sequence $W(k)$ to generate the output $b(k)$.

4.4 Error Analysis

Even with correction, the weight s_1 is not expected to be exactly the ideal solution. This section attempts to analyze the weight (s_1) error after correction compared to the ideal weight. Consider a simple case where only signals from the home base station and one interfering base station are present at the mobile station receiver. Then the signal vector at the array input of the mobile station is given by

$$\mathbf{r}(t) = [r_1(t), r_2(t)]^T, \tag{4.8}$$

The signal at two elements, $r_m(t)$ $(m = 1, 2)$ can be written as

$$\begin{aligned} r_m(t) &= c_{0m}(t)\sqrt{P_{0u}}\, d_{00}(t)W_{00}(t)u(t) + c_{0m}(t)\sqrt{P_{0u}}\sum_{k=1}^{K_0} d_{0k}(t)W_{0k}(t)u(t) \\ &\quad + c_{0m}(t)\sqrt{P_{0p}}u(t) + c_{1m}(t)\sqrt{P_{1u}}\sum_{k=0}^{K_1} d_{1k}(t-\tau_1-\tau_1')W_{1k}(t-\tau_1-\tau_1')\cdot \\ &\quad u(t-\tau_1-\tau_1') + c_{1m}(t)\sqrt{P_{1p}}\,u(t-\tau_1-\tau_1'), \end{aligned} \tag{4.9}$$

where the notations are the same as in (4.5), again $\tau_0 = \tau_0' = 0$, and the noise term is neglected. The first and second terms in (4.9) are the users' signals from the home base station; the third term is the home base station pilot; the fourth term is the users' signals from the interfering base station; and the fifth term is the interfering base station pilot. The signal $y(t)$ will contain the same terms modified by the weights s_1 and s_2. Therefore, if despreading of $y(t)$ is performed by correlating with the home base station pilot sequence $u(t)$, which is the home base station short code, then the first and second terms in (4.9) will be eliminated due to the zero average of the Walsh sequences $W_{0k}(t)$ $(k = 0, \cdots, K_0)$. For brevity, the contribution of the fourth term is neglected in the analysis, but will be discussed at the end of this section. Following this argument, in the sequel only the contribution corresponding to the third and the fifth terms in (4.9) will be considered, where the third term is our desired signal and the fifth term provides the interference. Assume that all channels keep constant during at least one symbol interval T_s. In the interest of brevity, the symbol index notation is ignored.

In step 2 of the algorithm, one of the hybrid inputs, x is obtained by weighting the input signal at the second element

$$\begin{aligned} x(n) &= s_1 \cdot r_2(n) \\ &= \sqrt{P_{0p}}\, s_1 c_{02} u(n) + \sqrt{P_{1p}}\, s_1 c_{12} u(n-\tau_1-\tau_1'), \end{aligned} \tag{4.10}$$

where the time index has also been omitted in c_{nm}, which are constant during the processing interval. The difference and sum signals at the output of the hybrid are

given respectively by

$$\begin{aligned} z(n) &= r_1(n) - x(n) \\ &= \sqrt{P_{0p}}\,(c_{01} - s_1 c_{02})\,u(n) + \sqrt{P_{1p}}\,(c_{11} - s_1 c_{12})\,u(n - \tau_1 - \tau_1'), \quad (4.11) \\ y_b(t) &= r_1(n) + x(n) \\ &= \sqrt{P_{0p}}\,(c_{01} + s_1 c_{02})\,u(n) + \sqrt{P_{1p}}\,(c_{11} + s_1 c_{12})\,u(n - \tau_1 - \tau_1'). \quad (4.12) \end{aligned}$$

The signal $y_a(n)$ provides an estimate of interference at $y_b(n)$, is given by

$$\begin{aligned} y_a(n) &= s_2 \cdot z(n) \\ &= \sqrt{P_{0p}}\,(c_{01} - s_1 c_{02}) s_2\,u(n) + \sqrt{P_{1p}}\,(c_{11} - s_1 c_{12}) s_2\,u(n - \tau_1 - \tau_1'), \quad (4.13) \end{aligned}$$

where s_2 is the DMI solution of the weight (see step 5 in the algorithm). Combining (4.12) and (4.13), one has the expression of the array output as follows

$$\begin{aligned} y(n) &= y_b(n) - y_a(n) \\ &= \alpha_0 u(n) + \alpha_1 u(n - \tau_1 - \tau_1'), \quad (4.14) \end{aligned}$$

where the quantities α_0 and α_1 are given by:

$$\alpha_0 = \sqrt{P_{0p}}\,(c_{01} + s_1 c_{02} - w c_{01} + s_1 s_2 c_{02})$$

$$\alpha_1 = \sqrt{P_{1p}}\,(c_{11} + s_1 c_{12} - w c_{11} + s_1 s_2 c_{12}).$$

It is noticeable that $|\alpha_0|$ and $|\alpha_1|$ are the amplitudes of the desired signal and interference at point y, respectively. After despreading, the output g_0 can be written as

$$g_0 = \alpha_0 + \alpha_1 \rho, \quad (4.15)$$

where it is assumed that $\frac{1}{N_p} \sum_{N_p} u^2(n) = 1$, and ρ is the correlation coefficient between home base station short code and interfering base station short code, with $\frac{1}{N_p} \sum_{N_p} u(n) u(n - \tau_1 - \tau_1') = \rho$. The reference signal is given by

$$\begin{aligned} g(n) &= g_0 u(n) \\ &= \alpha_0 u(n) + \alpha_1 \rho u(n). \quad (4.16) \end{aligned}$$

The control signals h_1 and h_2 calculated in steps 9 and 10 of the algorithm are given by

$$\begin{aligned} h_1 &= \frac{1}{N_p}\sum_{N_p} r_1(n)g^*(n) \\ &= \alpha_0^*\sqrt{P_{0p}}\,(c_{01}-s_1c_{02})+\alpha_1^*\sqrt{P_{1p}}\,(c_{11}-s_1c_{12})\,\rho^2 \\ &\quad +\alpha_1^*\sqrt{P_{0p}}(c_{01}-s_1c_{02})\rho+\alpha_0^*\sqrt{P_{1p}}(c_{11}-s_1c_{12})\rho, \qquad (4.17) \\ h_2 &= \frac{1}{N_p}\sum_{N_p} z(n)g^*(n) \\ &= \left(c_{01}\sqrt{P_{0p}}+c_{11}\rho\sqrt{P_{1p}}\right)(\alpha_0^*+\alpha_1^*\rho), \qquad (4.18) \end{aligned}$$

By using (4.17) and (4.18), the estimation of ideal weight s_1 in step 11 of the algorithm can be written as

$$\begin{aligned} \hat{s}_1 &= s_1+\frac{h_1}{h_2-h_1}\cdot s_1 \\ &= s_1\cdot\frac{h_2}{h_2-h_1} \\ &\approx \frac{s_1\left[c_{01}\sqrt{P_{0p}}(\alpha_0^*+\alpha_1^*\rho)+c_{11}\sqrt{P_{1p}}\alpha_0^*\rho\right]}{s_1\left[c_{02}\sqrt{P_{0p}}(\alpha_0^*+\alpha_1^*\rho)+c_{12}\sqrt{P_{1p}}\alpha_0^*\rho\right]+c_{11}\sqrt{P_{1p}}\alpha_1^*\rho}, \qquad (4.19) \end{aligned}$$

where the terms with ρ^2 are dropped since $\rho \ll 1$ in practice. As stated previously, the ideal weight s_1 should be set such that there is no signal power from home base station at point z, which means that the first term in (4.11) equals to zero, therefore, the ideal solution of s_1 in ith symbol interval is: $s_1(i) = c_{01}/c_{02}$. Hence, the error of the estimated ideal weight $\hat{s}_1(i)$ compared to the ideal weight is given by

$$\begin{aligned} \varepsilon &= \hat{s}_1-\frac{c_{01}}{c_{02}} \\ &\approx \frac{\left[(c_{11}c_{02}-c_{12}c_{01})\alpha_0^*-c_{11}c_{01}\alpha_1^*\right]\sqrt{P_{1p}}\,\rho}{c_{02}^2\alpha_0^*\sqrt{P_{0p}}}, \qquad (4.20) \end{aligned}$$

where the terms with ρ at the denominator are ignored. Eq.(4.20) gives the error expression when considering the effect of third and fifth terms in (4.9). If we also take into account the fourth term of (4.9), then the numerator in (4.20) should include

the items with $\sqrt{P_{1u}}\,\rho_k$ $(k = 0, \cdots, K_1)$, where ρ_k are the cross coefficients between home base station pilot sequence $u(t)$ and interfering signal spreading sequences $W_{1k}(t - \tau_1 - \tau_1')\,u(t - \tau_1 - \tau_1')$. Eq.(4.20) shows that higher home base station pilot power (P_{0p}), lower interfering signal power (P_{1p} and P_{1u}) and smaller cross-correlations (ρ and ρ_k) between the spreading codes result in less estimation error of beam steering weight. Especially, when ρ and $\rho_k \rightarrow 0$ (in case of orthogonal codes for example), the estimation error $\varepsilon \rightarrow 0$.

4.5 Multipath Solution

In the previous section, only a single path of each signal is assumed in the system. In terrestrial communication, the transmitted signal is reflected by a variety of smooth and rough terrains, so that it is replicated at the receiver with several time delays. Each individual path also arrives at its own amplitude and carrier phase. In this case, the received signal at the mobile station can be written as:

$$\mathrm{r}(t) = \sum_{j=0}^{J} \sum_{l=1}^{L} \mathbf{c}_{jl}(t) \left\{ \sum_{k=0}^{K_j} \sqrt{P_{ju}} \cdot d_{jk}(t - \tau_{jl}) u_{jk}(t - \tau_{jl}) + \sqrt{P_{jp}} \cdot u_j(t - \tau_{jl}) \right\} + \mathrm{v}(t), \tag{4.21}$$

where $\mathbf{c}_{jl}(t)$ represents the complex channel vector of the lth path and the jth base station, L is the number of resolvable paths and all other parameters are the same as in (4.5). Similar to the reverse link receiver, the RAKE receiver is used as the optimum demodulator structure for L multiple propagation paths. The combined smart antenna and RAKE receiver structure is shown in Figure 4.5, the scheme in Figure 4.4 is used for each of L parallel demodulators (RAKE fingers). The optimum demodulator forms the summation of weighted, phase-adjusted, and delay-adjusted L components, and makes final detection of the kth user's signal.

CDMA provides soft handoff. As the mobile station moves to the edge of its home cell, the adjacent base station assigns a modem to the call, while the current base station continues to handle the call. The call is handled by both base stations

on a make-before-break basis. The mobile station will receive the transmission from the two base stations as additional multipaths in the RAKE receiver and will process them as one signal. In the proposed smart antenna receiver, RAKE fingers search the strongest L paths from both base stations. In each finger only one path is demodulated as the desired signal, all others are treated as interference, which is similar to regular multipath combining. Therefore, the proposed receiver structure can also work well during the soft handoff.

4.6 Numerical Results

Computer simulations are used to show the operation of the proposed smart antenna, and to examine the receiver performance improvement due to the smart antenna. The following assumptions are made in the simulations:

1. Three resolvable paths for each signal are present, the relative delay between paths from the same base station is four chip intervals. In each of the RAKE fingers, there are one desired signal path and two interfering paths (self-interference) from home base station, as well as three interfering paths from each of six neighboring base stations.

2. The signals at two antenna elements have complex Gaussian channels with cross-correlation a.

3. Slow fading is assumes, and the channels are constant during one symbol interval T_s.

4. The distances between the mobile station and neighboring base stations D_j are modeled as uniformly distributed from R_0 to $3R_0$, where R_0 is the radius of the cell.

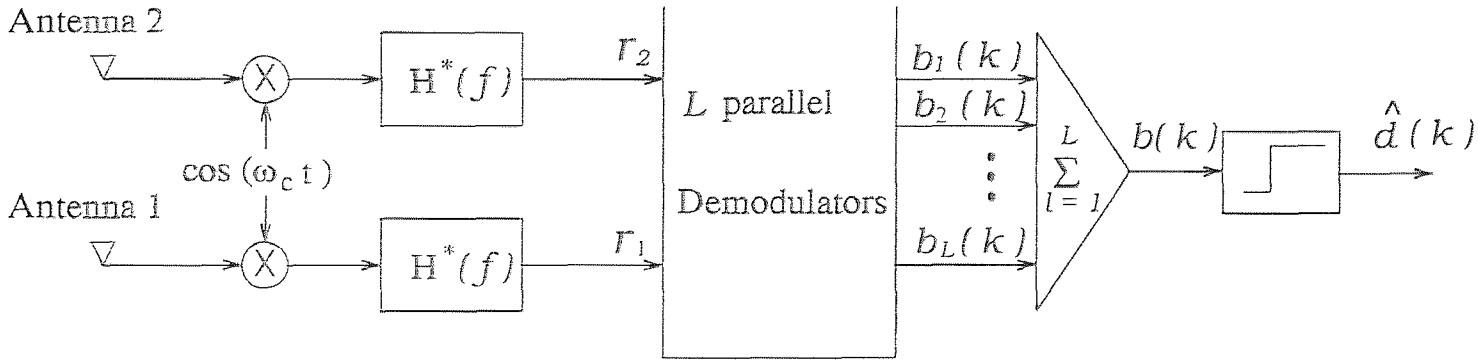

Figure 4.5 Smart antenna receiver at kth user's CDMA mobile station.

5. The distance between the mobile station and the home base station is $(2/3)R_0$, and the received signal power at the mobile station is proportional to $1/D_j^4$.

6. The short code is generated from the LFSR with tap polynomials in (4.1).

7. 20 percent of total transmitted power from each base station is used for pilot channel, the users' information channels equally share the other 80 percent of the transmitted power.

8. Assume no prior knowledge of the channel information, and the initial weight $s_1(0) = 1$.

To see clearly the performance improvement due to the proposed smart antenna receiver, we examine three different receiver models:

1. One antenna followed by RAKE demodulator.

2. Two antennas with maximal ratio combining (MRC) followed by RAKE demodulator.

3. Proposed smart antenna followed by RAKE demodulator.

In Figure 4.6, we assumed 20 active users per cell, the curves are obtained from 200 Monte Carlo runs. The signal channels at two antenna elements are assumed uncorrelated ($a = 0$). For receivers 1 and 2, the curves depict the average output SINR over symbols 1 to 20. For the receiver with smart antenna, the curve depicts the output SINR at $b(k)$ of Figure 4.5 is averaged over symbols 1 to 5, while taking the initial beam steering weight $s_1 = 1$. Starting from symbol 6, the smart antenna uses the proposed algorithm to control the weight s_1, and the output SINR is averaged over symbols 6 to 20. This curve shows that after the weight (s_1) correction starts, the receiver with the proposed smart antenna achieves 1.5 dB and 3.5 dB higher output SINR compared to receivers 1 and 2, respectively.

To see the capacity improvement due to the proposed receiver with smart antenna, Figure 4.7 depicts the simulation results of probability of symbol error, P_e, versus number of users per cell, where the voice activity is assumed to be 37.5%. For performance requirement $P_e = 10^{-2}$, the system capacity is 22, 35 and 43 users per cell for receivers 1, 2 and 3, respectively. That is, with receiver 3, the system capacity increases by 95% and 23% compared to receivers 1 and 2, respectively.

Next, we examine the effect of correlation between the received signals at two antenna elements. Figure 4.8 shows the results for correlation coefficients $a = 0.3$ and 0.6. For comparison, the results with $a = 0$ are also plotted. The figure depicts that even with $a = 0.3$ and 0.6, the performance of receiver 3 is almost the same as in the case of $a = 0$ (cannot be distinguished in the figure), while the output SINR of receiver 2 degrades by 0.3 dB and by 0.9 dB, respectively.

The effect of mobile station movement is also studied. Here the fading is modeled by the autoregressive (AR) process (see [51] for details): $\mathbf{c}_j(i+1) = \beta \mathbf{c}_j(i) + \Delta(i)$, where $0 < \beta < 1$, and $\Delta(i)$ is AWGN with variance of corresponding element $(1-\beta^2)|c_{jm}(0)|^2$. For the mobile station speeds of 30 mph and 60 mph, β becomes 0.995 and 0.986 respectively, while other conditions stay unchanged. Since the channel estimate is performed at each symbol, Figure 4.9 shows that even for a fast moving mobile station ($v = 60$ mph), the proposed receiver can also obtain the same performance as for stationary mobile station.

4.7 Summary

Adaptive antenna array application for interference suppression at the mobile station of a wireless CDMA system was studied. A new algorithm utilizing home base station short code to generate a reference signal was proposed. The algorithm, besides facilitating interference suppression, adaptively controls the beam steering weight and thus overcomes the channel estimation error. It was shown that the beam

steering weight error could be substantially reduced by this algorithm, and averaging only on part of the PN short code has small effect. Numerical results were presented to illustrate the operation of the algorithm and the improvement of performance.

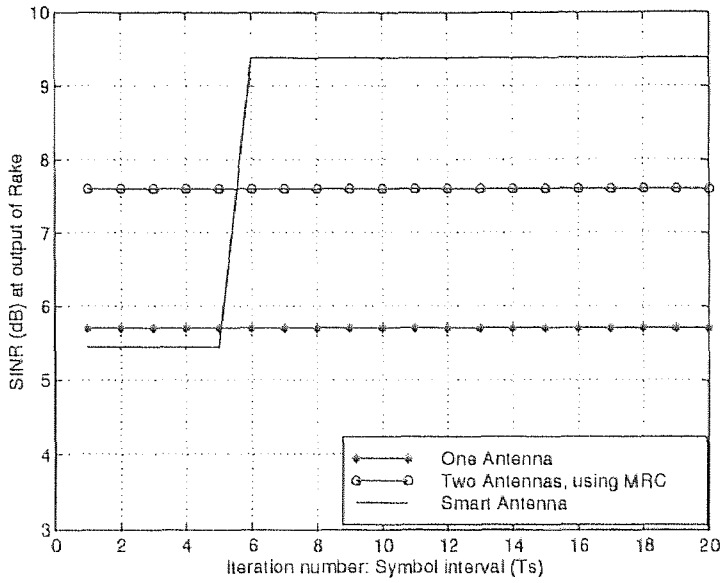

Figure 4.6 Output SINR versus iteration number with $a = 0$ and $v = 0$ mph

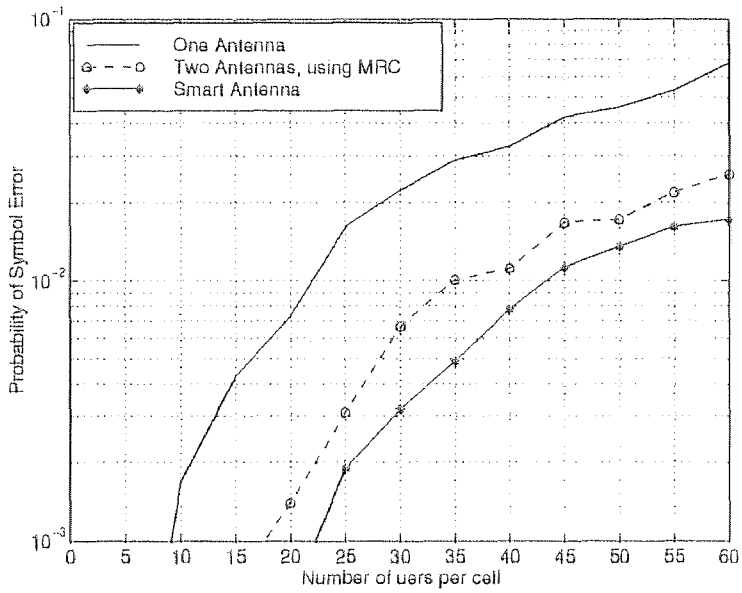

Figure 4.7 Probability of symbol error versus number of users per cell with $a = 0$ and $v = 0$ mph

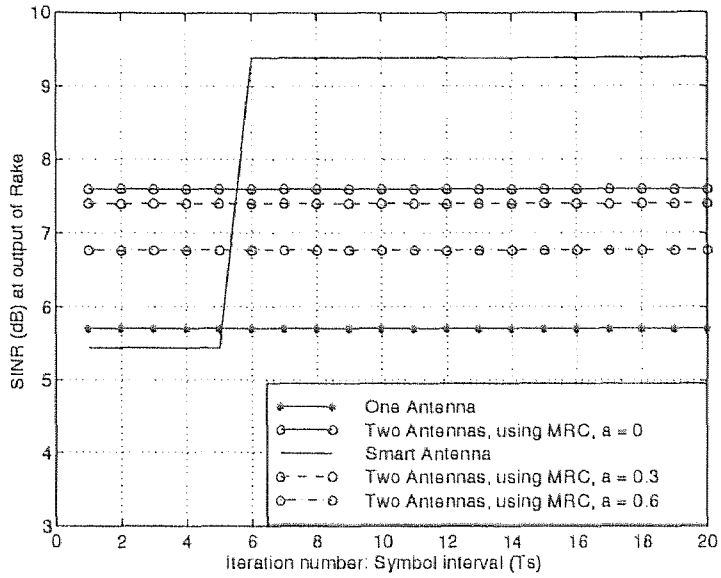

Figure 4.8 Output SINR versus iteration number with $a = 0$, 0.3 and 0.6, $v = 0$ mph

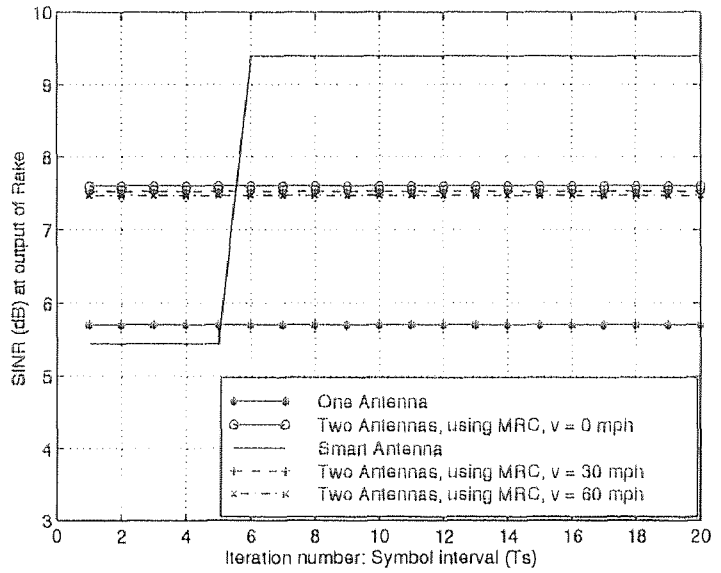

Figure 4.9 Output SINR versus iteration number with $a = 0$, $v = 0$, 30 and 60 mph

CHAPTER 5
CONCLUSIONS

In this dissertation, applications of adaptive antenna arrays in wireless CDMA were studied. Adaptive antenna arrays along with RAKE receivers provide space-time processing, improves the CDMA system performance, and increases both the reverse link and forward link capacity.

In Chapter 2, the system model of space-time adaptive processing in the reverse link receiver was introduced. Two combining methods in joint space and time domains were considered in the analysis. MRC maximizes the output SNR, while OC maximizes SINR. The asymptotic efficiency and its worst case result, known as near-far resistance, were analyzed and their analytical expressions were derived. It was shown that while MRC is not near-far resistant, joint domain OC is near-far resistant when the number of cochannel interference sources is less than the degrees of STAP freedom. The STAP with OC can mitigate the CCI and thus improve the system performance.

More detailed reverse link performance analyses were carried out in Chapter 3, where the system performance was analyzed in terms of outage probability and probability of bit error. Two different definitions of the outage were used in the analyses, one is for the instantaneous SIR, the other for the average SIR. The performance analyses included the following effects: STAP (joint domain MRC), Rayleigh fading, PCE, voice activity, other cell interference, correlated shadowing, and pilot tone. The system capacity could be obtained in terms of both the number of users per cell and Erlang per cell. New analytical expressions were derived and verified by computer simulations. The results showed the performance loss due to PCE and performance improvement by STAP.

Application of STAP in the forward link receiver was investigated in Chapter 4, where a novel receiver with smart antenna (two antenna elements) followed by a

RAKE demodulator at the mobile station was proposed for interference suppression and diversity combining. For the specific application of IS-95A CDMA, a new algorithm was developed to utilize the pilot signal for adaptive control of the beam steering weight and thus overcome the channel estimation error. Computer simulations showed that the proposed smart antenna structure outperforms the one antenna receiver as well as the two-antenna receiver with MRC, and the capacity improvement with 1% BER was 95% and 23%, respectively (two antennas are uncorrelated). With certain correlation between the two antennas, output SINR of two-antenna receiver with MRC degraded while the proposed smart antenna receiver had no performance loss.

Based on above studies of STAP, it is concluded that adaptive antenna arrays could be among the strongest candidates for further capacity improvement of wireless CDMA systems. The exploitation of STAP is under active research in both research institutions and industry. It is expected that adaptive antenna array will be one of the key elements for system performance improvement in the next generation wireless communication infrastructure.

APPENDIX A

DERIVATION OF THE NEAR-FAR RESISTANCE OF THE JOINT DOMAIN OPTIMUM COMBINING

This appendix derives the expressions given in (2.25) and (2.26). Utilizing (2.24), one has

$$\begin{aligned}
\lim_{\sigma^2 \to 0} \|\mathbf{w}\|^2 &= \lim_{\sigma^2 \to 0} \mathbf{w}^H \mathbf{w} \\
&= \mathbf{c}_0^H \left(\mathbf{I} - \sum_{k=1}^{K} \frac{\mathbf{c}_k \mathbf{c}_k^H}{\|\mathbf{c}_k\|^2} \right) \left(\mathbf{I} - \sum_{k=1}^{K} \frac{\mathbf{c}_k \mathbf{c}_k^H}{\|\mathbf{c}_k\|^2} \right) \mathbf{c}_0 \\
&= \mathbf{c}_0^H \left(\mathbf{I} - 2 \sum_{k=1}^{K} \frac{\mathbf{c}_k \mathbf{c}_k^H}{\|\mathbf{c}_k\|^2} + \sum_{k=1}^{K} \frac{\mathbf{c}_k \mathbf{c}_k^H \mathbf{c}_k \mathbf{c}_k^H}{\|\mathbf{c}_k\|^4} \right) \mathbf{c}_0 \\
&= \mathbf{c}_0^H \left(\mathbf{I} - \sum_{k=1}^{K} \frac{\mathbf{c}_k \mathbf{c}_k^H}{\|\mathbf{c}_k\|^2} \right) \mathbf{c}_0 \\
&= \|\mathbf{c}_0\|^2 - \sum_{k=1}^{K} \frac{|\mathbf{c}_0^H \mathbf{c}_k|^2}{\|\mathbf{c}_k\|^2}, \qquad \text{(A.1)}
\end{aligned}$$

where the assumption of orthogonality in (2.16) is applied.

To derive the result of (2.26), we use the expression of (2.18). The second term in the $\max(\cdot)$ function of (2.18) can be calculated as

$$\begin{aligned}
\lim_{\sigma^2 \to 0} \left(\left| \mathbf{w}^H \mathbf{c}_0 \right| - \sum_{k=1}^{K} \frac{A_k \left| \mathbf{w}^H \mathbf{c}_k \right|}{A_0} \right) &= \left| \mathbf{c}_0^H \left(\mathbf{I} - \sum_{k=1}^{K} \frac{\mathbf{c}_k \mathbf{c}_k^H}{\|\mathbf{c}_k\|^2} \right) \mathbf{c}_0 \right| \\
&\quad - \sum_{k=1}^{K} \frac{A_k}{A_0} \left| \mathbf{c}_0^H \left(\mathbf{I} - \sum_{k=1}^{K} \frac{\mathbf{c}_k \mathbf{c}_k^H}{\|\mathbf{c}_k\|^2} \right) \mathbf{c}_k \right| \\
&= \left| \mathbf{c}_0^H \mathbf{c}_0 - \sum_{k=1}^{K} \frac{\mathbf{c}_k \mathbf{c}_k^H}{\|\mathbf{c}_k\|^2} \right| - \sum_{k=1}^{K} \frac{A_k}{A_0} \left| \mathbf{c}_0^H \mathbf{c}_k - \sum_{k=1}^{K} \mathbf{c}_0^H \mathbf{c}_k \right| \\
&= \left| \|\mathbf{c}_0\|^2 - \sum_{k=1}^{K} \frac{|\mathbf{c}_0^H \mathbf{c}_k|^2}{\|\mathbf{c}_k\|^2} \right| \\
&= \lim_{\sigma^2 \to 0} \|\mathbf{w}\|^2. \qquad \text{(A.2)}
\end{aligned}$$

Since the result in (A.2) is always greater than or equal to zero, the $\max(\cdot)$ expression in (2.18) is just equal to the second term. Thus, the near-far resistance of the joint

domain OC expressed in (2.18) can be written as

$$\begin{aligned}
\overline{\eta} &= \lim_{\substack{\sigma^2 \to 0 \\ A_k \to \infty}} \frac{\left[\max\left(0, |\mathbf{w}^H \mathbf{c}_0| - \sum_{k=1}^{K} \frac{A_k |\mathbf{w}^H \mathbf{c}_k|}{A_0}\right)\right]^2}{\|\mathbf{c}_0\|^2 \|\mathbf{w}\|^2} \\
&= \lim_{\substack{\sigma^2 \to 0 \\ A_k \to \infty}} \frac{\left(|\mathbf{w}^H \mathbf{c}_0| - \sum_{k=1}^{K} \frac{A_k |\mathbf{w}^H \mathbf{c}_k|}{A_0}\right)^2}{\|\mathbf{c}_0\|^2 \|\mathbf{w}\|^2} \\
&= \frac{\|\mathbf{w}\|^4}{\|\mathbf{c}_0\|^2 \|\mathbf{w}\|^2} \\
&= 1 - \sum_{k=1}^{K} \frac{|\mathbf{c}_0^H \mathbf{c}_k|^2}{\|\mathbf{c}_0\|^2 \|\mathbf{c}_k\|^2},
\end{aligned} \tag{A.3}$$

which is the result in (2.26).

APPENDIX B

DERIVATION OF AVERAGE SIGNAL POWER AND INTERFERENCE POWER OVER RAYLEIGH FADING

This appendix derives the expressions in (3.30) and (3.33). The expectation expression at the right hand side of (3.29) can be written as

$$\begin{aligned} E\left[\left(\sum_{m=1}^{M}|c_{1m}|^2\right)^2\right] &= E\left[\left(\sum_{m=1}^{M}|c_{1m}|^2\right)\left(\sum_{i=1}^{M}|c_{1i}|^2\right)\right] \\ &= E\left[\sum_{m=1}^{M}|c_{1m}|^4 + 2\sum_{m=1}^{M-1}\sum_{i=m+1}^{M}|c_{1m}|^2|c_{1i}|^2\right] \\ &= E\left[\sum_{m=1}^{M}|c_{1m}|^4\right] + 2\sum_{m=1}^{M-1}\sum_{i=m+1}^{M}E\left[|c_{1m}|^2|c_{1i}|^2\right]. \end{aligned} \quad (B.1)$$

The first term in (B.1) is given by

$$\begin{aligned} E\left[\sum_{m=1}^{M}|c_{1m}|^4\right] &= \sum_{m=1}^{M}E\left[|c_{1m}|^4\right] \\ &= M\,E\left[|c_{11}|^4\right], \end{aligned} \quad (B.2)$$

where we used the assumption that c_{1m} are i.i.d. RVs. Since the channel coefficient c_{11} is assumed to be a complex symmetric Gaussian RV, with zero mean and $E[|c_{11}|^2]=1$, one can write $c_{11}=c_{11R}+jc_{11I}$, where c_{11R} and c_{11I} are i.i.d. Gaussian RV $\sim\mathcal{N}(m_c,\sigma_c^2)$ with $m_c=0$ and $\sigma_c^2=\frac{1}{2}$. Therefore,

$$|c_{11}|^2 = c_{11R}^2 + c_{11I}^2,$$

and

$$\begin{aligned} E\left[|c_{11}|^4\right] &= E\left[\left(c_{11R}^2+c_{11I}^2\right)^2\right] \\ &= E\left[c_{11R}^4 + c_{11I}^4 + 2c_{11R}^2\,c_{11I}^2\right] \\ &= 2E\left[c_{11R}^4\right] + 2E\left[c_{11R}^2\right]E\left[c_{11I}^2\right] \\ &= 2E\left[c_{11R}^4\right] + \frac{1}{2}. \end{aligned} \quad (B.3)$$

The fourth moment of Gaussian RV c_{11R} is given by

$$\begin{aligned} E\left[c_{11R}^4\right] &= m_c^4 + 6m_c^2\sigma_c^2 + 3\sigma_c^4 \\ &= \frac{3}{4}. \end{aligned} \tag{B.4}$$

Substituting (B.4) into (B.3), one has

$$E\left[|c_{11}|^4\right] = 2. \tag{B.5}$$

Thus the first term in (B.1) is

$$E\left[\sum_{m=1}^{M} |c_{1m}|^4\right] = 2M. \tag{B.6}$$

The second term in (B.1) can be written as

$$\begin{aligned} 2\sum_{m=1}^{M-1}\sum_{i=m+1}^{M} E\left[|c_{1m}|^2 |c_{1i}|^2\right] &= 2\sum_{m=1}^{M-1}\sum_{i=m+1}^{M} E\left[|c_{1m}|^2\right] E\left[|c_{1i}|^2\right] \\ &= M(M-1). \end{aligned} \tag{B.7}$$

Applying (B.6) and (B.7) in (B.1), one has

$$\begin{aligned} E\left[\left(\sum_{m=1}^{M} |c_{1m}|^2\right)^2\right] &= 2M + M(M-1) \\ &= M^2 + M. \end{aligned} \tag{B.8}$$

Using (B.8) in (3.29), one obtains (3.30).

For the expression in (3.33), we have

$$\begin{aligned} J &= \mathcal{I}\, E\left[\left|\mathbf{c}_1^H \mathbf{e}_p\right|^2\right] \\ &= \mathcal{I}\, E\left[\left|\sum_{m=1}^{M} c_{1m}^* c_{pm}\right|^2\right] \\ &= \mathcal{I} E\left[\left(\sum_{m=1}^{M} c_{1m}^* c_{pm}\right)\left(\sum_{i=1}^{M} c_{1i} c_{pi}^*\right)\right] \\ &= \mathcal{I} E\left[\sum_{m=1}^{M} |c_{1m}|^2 |c_{pm}|^2\right] + \mathcal{I} E\left[2\sum_{m=1}^{M-1}\sum_{i=m+1}^{M} c_{1m}^* c_{pm} c_{1i} c_{pi}^*\right]. \end{aligned} \tag{B.9}$$

Since c_{1m}, c_{pm}, c_{1i} and c_{pi} $(i \neq m)$ are independent Gaussian RVs, with zero mean, the second term in (B.9) is equal to zero. Thus

$$\begin{aligned} J &= \mathcal{I}E\left[\sum_{m=1}^{M} |c_{1m}|^2 |c_{pm}|^2\right] \\ &= \mathcal{I}\sum_{m=1}^{M} E\left[|c_{1m}|^2\right] E\left[|c_{pm}|^2\right] \\ &= M\mathcal{I}. \end{aligned} \tag{B.10}$$

APPENDIX C

GLOSSARY OF ABBREVIATIONS

AMPS: advanced mobile phone system

AR: autoregressive

ARQ: automatic repeat request

AWGN: additive white Gaussian noise

BER: bit error rate

BPSK: binary phase-shift keying

CCI: cochannel interference

CDF: cumulative distribution function

CDMA: code-division multiple access

DMI: direct matrix inversion

FDMA: frequency-division multiple access

GPS: global positioning system

GSC: generalized sidelobe canceller

i.i.d.: independent identically distributed

LMS: least mean square

LFSR: linear feedback shift register

MIL: matrix inversion lemma

MLSR: maximum-length shift-register

MRC: maximal ratio combining

NRZ: nonreturn-to-zero

OC: optimum combining

PCE: power control error

PCS: personal communications systems

PDF: probability density function

PN: pseudo-noise

RLS: recursive least square

RV: random variable

SINR: signal-to-interference plus noise ratio

SIR: signal-to-interference ratio

SNR: signal-to-noise ratio

STAP: space-time adaptive processing

TDMA: time-division multiple access

REFERENCES

1. V. K. Garg, K. Smolik, and J. E. Wilkes, *Applications of CDMA in Wireless/Personal Communications*, Prentice Hall PTR, Upper Saddle River, NJ, 1997.

2. J. D. Gibson, *The Mobile Communications Handbook*, CRC Press, Inc., Boca Raton, FL, 1996.

3. D. L. Schilling, "Wireless communications going into the 21st century," *IEEE Trans. Vehicular Tech.*, vol. 43, pp. 645–652, Aug. 1994.

4. A. M. Viterbi and A. J. Viterbi, "Erlang capacity of a power controlled CDMA system," *IEEE J. Select. Areas Commun.*, vol. 11, pp. 892–900, Aug. 1993.

5. K. S. Gilhousen, I. M. Jacobs, R. Padovani, A. J. Viterbi, L. A. Weaver, and C. E. Wheatley, "On the capacity of a cellular CDMA system," *IEEE Trans. Vehicular Technology*, vol. 40, pp. 303–312, May 1991.

6. A. J. Viterbi, "Wireless digital communication: a view based on three lessons learned," *IEEE Communications Magazine*, pp. 33–36, Sept. 1991.

7. V. K. Garg and L. Huntington, "Applications of adaptive array antenna to a TDMA cellular/PCS system," *IEEE Communications Magazine*, pp. 148–152, Oct. 1997.

8. G. Tsoulos, M. Beach, and J. McGeehan, "Wireless personal communications for the 21st century: European technological advances in adaptive antennas," *IEEE Communications Magazine*, vol. 35, pp. 102–109, Sept. 1997.

9. J. Litva, *Digital Beamforming in Wireless Communications*, Artech House, Inc., Norwood, MA, 1996.

10. J. H. Winters, "Optimum combining in digital mobile radio with cochannel interference," *IEEE J. Select. Areas Commun.*, vol. 4, pp. 528–539, July 1984.

11. J. H. Winters, "Optimum combining for indoor systems with multiple users," *IEEE Trans. communications.*, vol. 35, pp. 1222–1230, Nov. 1987.

12. J. H. Winters, "The impact of antenna diversity on the capacity of wireless communication systems," *IEEE Trans. communications.*, vol. 42, pp. 1740–1751, Feb./Mar./Apr. 1994.

13. A. F. Naguib and A. Paulraj, "Performance of CDMA cellular networks with base-station antenna arrays," Zurich, Switzerland, pp. 87–100, Mar. 1994.

14. X. C. Bernstein and A. M. Haimovich, "Space-time optimum combining for CDMA communications," *Wireless Personal Communications*, vol. 3, pp. 73–89, 1996.

15. A. F. Naguib and A. Paulraj, "Performance of wireless CDMA with M-ary orthogonal modulation and cell site antenna arrays," *IEEE J. Select. Areas Commun.*, vol. 14, pp. 1770–1783, Dec. 1996.

16. B. Sklar, "Rayleigh fading channels in mobile digital communication systems, Part I: Charaterization," *IEEE Communications Magazine*, pp. 90–100, July 1997.

17. J. G. Proakis, *Digital Communications*, McGraw-Hill, Inc., New York, NY, 1995.

18. A. J. Viterbi, *CDMA Principles of Spread Spectrum Communication*, Addison-Wesley Publishing Company, Reading, MA, 1995.

19. W. C. Jakes, *Microwave Mobile Communications*, John Wiley & Sons, New York, 1974.

20. T. S. Rappaport, *Wireless Communications: Principles and Practice*, Prentice Hall PTR, Upper Saddle River, NJ, 1996.

21. S. Verdu, "Optimum multiuser asymptotic efficiency," *IEEE Trans. on Communications*, vol. 34, pp. 890–897, Sept. 1986.

22. R. Lupas and S. Verdu, "Near-far resistance of multiuser detection in asymptotic channels," *IEEE Trans. on Communications*, vol. 38, pp. 496–508, Apr. 1990.

23. S. Moshavi, "Multi-user detection for DC-CDMA communications," *IEEE Communications Magazine*, pp. 124–136, Oct. 1996.

24. J. D. Laster and J. H. Reed, "Interference rejection in digital wireless communications," *IEEE Signal Processing Magazine*, pp. 37–62, May 1997.

25. R. Padovani, "Reverse link performance of IS-95 based cellular systems," *IEEE Personal Communications Magazine*, pp. 28–34, Third Quarter 1994.

26. N. A. Marlow, "A normal limit theorem for power sums of independent random variables," *The Bell System Technical Journal*, vol. 46, pp. 2081–9, Nov. 1967.

27. S. C. Schwartz and Y. S. Yeh, "On the distribution function and moments of power sums with log-normal components," *The Bell System Technical Journal*, vol. 61, pp. 1441–1462, Sept. 1982.

28. A. Safak, "Statistical analysis of the power sum of multiple correlated log-normal components," *IEEE Trans. Vehicular Technology*, vol. 42, pp. 58–61, Feb. 1993.

29. A. A. Abu-Dayya and N. C. Beaulieu, "Outage probability in the presence of correlated lognormal interferers," *IEEE Trans. Vehicular Technology*, vol. 43, pp. 164–173, Feb. 1994.

30. Y. S. Yeh and S. C. Schwartz, "Outage probability in mobile telephony due to multiple log-normal interferers," *IEEE Trans. communications.*, vol. 32, pp. 380–388, Apr. 1984.

31. A. J. Viterbi, A. M. Viterbi, and E. Zehavi, "Performance of power-controlled wideband terrestrial digital communication," *IEEE Trans. communications.*, vol. 41, pp. 559-569, Apr. 1993.

32. M. Soleimanipour and G. H. Freeman, "A realistic approach to the capacity of cellular CDMA systems," in *IEEE 46th Vehicular Technology Conference Proceedings*, Atlanta, GA, pp. 1125–9, Apr.28 - May 1 1996.

33. M. Zorzi and S. Pupolin, "Outage probability in multiple access interference radio networks in the presence of fading," *IEEE Trans. Vehicular Technology*, vol. 43, pp. 604–610, Aug. 1994.

34. M. Zorzi, "On the analytical computation of the interference statistics with applications to the performance evaluation of mobile radio systems," *IEEE Trans. communications.*, vol. 45, pp. 103 109, Jan. 1997.

35. A. F. Naguib, "Power control in wireless CDMA: performance with cell site antenna arrays," in *Proceedings of IEEE 1995 Global Telecommunications Conference*, Singapore, pp. 225–229, Nov. 1995.

36. B. R. Vojcic, R. L. Pickholtz, and L. B. Milstein, "Erlang capacity of a power controlled CDMA system," *IEEE J. Select. Areas Commun.*, vol. 12, pp. 560 -567, May 1994.

37. F. Vatalaro, G. E. Corazza, F. Ceccarelli, and G. D. Maio, "A realistic approach to the capacity of cellular CDMA systems," in *IEEE 46th Vehicular Technology Conference Proceedings*, Atlanta, GA, pp. 1125 9, Apr.28-May 1 1996.

38. N. Kong and L. B. Milstein, "Approximations to and chernoff bound on the error probabilities of multicell CDMA over a multipath fading channel with power control error," in *Proceedings of the 1996 Conference on Information Science and Systems*, Princeton, NJ, pp. 1131 1135, Mar. 1996.

39. S. P. Applebaum and D. J. Chapman, "Adaptive arrays with main beam constraints," *IEEE Trans. Antennas Propagat.*, vol. 24, pp. 650–662, September 1976.

40. R. T. Compton, Jr. "An adaptive array in spread-spectrum communications," *Proc. IEEE.*, vol. 66, pp. 289–298, Mar. 1978.

41. R. T. Compton, Jr. "Pointing accuracy and dynamic range in a steered beam array," *IEEE Trans. Aerospace and Electronic Systems.*, vol. 16, pp. 280–287, May 1980.

42. C. Yeh, F. Haber, and Y. Bar-Ness, "Effects of random amplitude and steering phase errors on the behavior of the hybrid array," in *Proceedings of GLOBECOM'84*, Atlanta, GA, pp. 184–188, Nov. 1984.

43. Y. Bar-Ness and F. Haber, "Self-correcting interference cancelling processor for point-to-point communications," in *Proceedings of the 24th Midwest Symposium on Circuit and Systems*, Albuquerque, NM, pp. 663–665, June 1981.

44. L. J. Griffiths and C. W. Jim, "An alternative approach to linearly constrained adaptive beamforming," *IEEE Trans. Antennas Propagat.*, vol. 30, pp. 27–34, January 1982.

45. N. K. Jablon, "Steady state analysis of the generalized sidelobe canceler by adaptive noise cancelling techniques," *IEEE Trans. Antennas Propagat.*, vol. 34, pp. 330–337, March 1986.

46. W. Ye, Y. Bar-Ness, and A. M. Haimovich, "A self-correcting loop for joint estimation-calibration in adaptive radar," in *Proceedings of the 1997 IEEE National Radar Conference*, Syracuse, NY, May 1997.

47. R. A. Monzingo and T. W. Miller, *Introduction to Adaptive Arrays*, John Wiley & Sons, NY, 1980.

48. A. Leon-Garcia, *Probability and Random Processes for Electrical Engineering*, Addison-Wesley Publishing Company, Reading, MA, 1994.

49. A. J. Claus, T. T. Kadota, and D. M. Romain, "Efficient approximation of a family of noises for application in adaptive spatial processing for signal detection," *IEEE Trans. Information Theory.*, vol. 26, pp. 588–595, Sept. 1980.

50. M. Thoma and A. Wyner, *Lecture Notes in Control and Information Sciences*, Springer-Verlag, Berlin, Germany, 1991.

51. X. C. Bernstein, "Adaptive space-time processing for wireless communications," Ph.D. dissertation, ECE Dept., New Jersey Inst. of Tech., Newark, NJ, Jan. 1996.

52. J. M. Holtzman, "A simple, accurate method to calculate spread-spectrum multiple-access error probabilities," *IEEE Trans. communications.*, vol. 40, pp. 461–464, Mar. 1992.

53. L. B. Milstein, T. S. Rappaport, and R. Barghouti, "Performance evaluation for cellular CDMA," *IEEE J. Select. Areas Commun.*, vol. 10, pp. 680–689, May 1992.

54. N. Kong and L. B. Milstein, "Performance of multicell CDMA with power control error," in *Proceedings of IEEE 1995 Military Communications Conference*, San Diego, CA, pp. 513–517, Nov. 1995.

55. A. Shah, "Adaptive space-time processing for digital mobile radio communication systems," Ph.D. dissertation, ECE Dept., New Jersey Inst. of Tech., Newark, NJ, May 1997.

56. J. B. Seaborn, *Hypergeometric Functions and Their Applications*, Springer-Verlag New York Inc., New York, NY, 1991.